Advanced Radar Technology for Wide Area Surveillance and Fire Control Quality Tracking

MITRE

Advanced Radar Technology for Wide Area Surveillance and Fire Control Quality Tracking

Study Leader:
J. Vesecky

Contributors Include:
A. Despain
R. Garwin
W. Nierenberg
O. Rothaus
J. Sullivan
R. Westervelt

January 1998

JSR-95-230

JASON
The MITRE Corporation
1820 Dolley Madison Boulevard
McLean, Virginia 22102-3481
(703) 883-6997

REPORT DOCUMENTATION PAGE

Form Approved
OMB No. 0704-0188

1. AGENCY USE ONLY (Leave blank)	2. REPORT DATE	3. REPORT TYPE AND DATES COVERED
	January 7, 1997	

4. TITLE AND SUBTITLE

Advanced Radar Technology for Wide Area Surveillance and Fire Control Quality Tracking

5. FUNDING NUMBERS

13-988534-04

6. AUTHOR(S)

J. Vesecky, A. Despain, R. Garwin, W. Nierenberg, O. Rothaus, J. Sullivan, R. Westervelt

7. PERFORMING ORGANIZATION NAME(S) AND ADDRESS(ES)

The MITRE Corporation
JASON Program Office
1820 Dolley Madison Blvd
McLean, Virginia 22102

8. PERFORMING ORGANIZATION REPORT NUMBER

JSR-95-230

9. SPONSORING/MONITORING AGENCY NAME(S) AND ADDRESS(ES)

Office of Naval Research
Code 111
800 North Quincy Street
Arlington, Virginia 22217

10. SPONSORING/MONITORING AGENCY REPORT NUMBER

JSR-95-230

11. SUPPLEMENTARY NOTES

12a. DISTRIBUTION/AVAILABILITY STATEMENT

Approved for public release; distribution unlimited.

12b. DISTRIBUTION CODE

Distribution Statement A

13. ABSTRACT *(Maximum 200 words)*

This report contains the results of the JASON summer study review of the ONR Advanced Capability Initiative (ACI) in Wide Area Surveillance and Fire Control Quality Tracking. The mission of this ACI is to identify and develop advanced technologies needed for new ship and airborne search, tracking and illumination radars that would give ships a more effective self-defense capability against very low altitude cruise missiles and aircraft.

14. SUBJECT TERMS

15. NUMBER OF PAGES

16. PRICE CODE

17. SECURITY CLASSIFICATION OF REPORT	18. SECURITY CLASSIFICATION OF THIS PAGE	19. SECURITY CLASSIFICATION OF ABSTRACT	20. LIMITATION OF ABSTRACT
Unclassified	Unclassified	Unclassified	SAR

Contents

ACKNOWLEDGEMENTS

We are pleased to acknowledge the help of a number of scientists and engineers from the Office of Naval Research, the Naval Research Laboratory and other organizations. In particular we are grateful for the encouragement, support and technical expertise of Dr. Bobby Junker of ONR and his colleagues Jim Hall, Bill Miceli and Max Yoder. Further, we thank Prof. John Volakis of the University of Michigan for help in the area of numerical electromagnetics applications to patch antennas.

1 INTRODUCTION AND OBJECTIVES

This report contains the results of the JASON summer study review of the ONR Advanced Capability Initiative (ACI) in Wide Area Surveillance and Fire Control Quality Tracking. The mission of this ACI is to identify and develop advanced technologies needed for new ship and airborne search, tracking and illumination radars that would give ships a more effective self-defense capability against very low altitude cruise missiles and aircraft.

1.1 Threat Background

Important Navy assets are threatened by sea skimming cruise missiles having very low radar cross sections and speeds in the mach one to mach three range. The Falkland Islands War of 1981 showed that a country with limited military power could acquire such missiles and use them effectively. The loss of the British destroyer Sheffield to an air-launched Exocet missile, 40 miles south of Port Stanley, Falkland Is., shocked Britain and had a political and morale impact far beyond the loss of a single ship. Events in the Persian Gulf, e.g. the missile attack on the USS Stark, have further illuminated the need for improved ship defense against missile attack, especially for ships near enemy shores. Current detection, tracking and targeting assets are highly stressed by the short response time provided by a mast head radar with an horizon only some 15 nautical miles (nm) away. The requirements on such a radar are to detect at the radar horizon, track the target to allow command control guidance of a Standard Missile 2 (SM-2) to within 3 to 4 nm of the target and then illuminate the SM-2 and target to allow the missile to use semi-active radar homing to intercept the target. For a Mach 1

incoming missile these functions must take place in less than 90 seconds and for a Mach 3 incoming missile in less than 30 seconds.

Clearly an advanced airborne radar that performs the above functions and extends the observational horizon out to some 200 nm would be extremely useful. Such a capability would allow a shoot-look-shoot approach and sufficient time to avoid targeting mistakes. An advanced radar will need to cope with very low cross section targets and high clutter situations, such as those found when mountains are within the radar field of view. We also note that in looking at the potential of airborne radars one should not neglect studies as to how much benefit could be obtained from better use of the time provided by mast-top radars.

1.2 ONR Advanced Capability Initiative (ACI) Overview

The ONR Advanced Capability Initiative (ACI) in Wide Area Surveillance and Fire Control Quality Tracking uses the advanced airborne radar discussed above as an organizing principle for a diverse set of research and development programs that seek to identify and support advanced technologies that can contribute to improved microwave radar performance over the next 5 to 10 years. In summary the mission of this ONR ACI is to identify and develop advanced technologies needed for an airborne search, tracking and illumination radar that gives ships a more effective self-defense capability against very low altitude cruise missiles and aircraft.

1.3 General Comments

First, we recognize the need for focussed, not general, systems level studies to go along with the development of advanced technology – we are more specific regarding system issues below and in the summary and conclusions (Section 6) at the end. Such studies both insure that appropriate technologies are selected for development and set priorities in terms of the impact of a given technology on overall system performance. System studies should also consider the side effects of a particular technology. This ACI properly includes both short and long range research. A mechanism is needed to integrate the near term technologies into actual radars for test in the real-life ocean clutter environment.

Phased array antennas use thousands of array elements, each of which is expensive – thousands of dollars. To lower the cost of such antennas it makes sense to invest significantly in lowering the manufacturing costs of the array elements. To illustrate this leverage consider the purchase of 100 antennas with 5000 elements each, thus a total of 500,000 array elements. Because of the large number of elements it makes economic sense to invest up to $5,000,000 to lower the cost of an element by only $10.

1.4 JASON summer study objectives

We considered a broad range of advanced radar technologies with the primary objective of commenting on these technologies and their role in a high capability radar, relevant to defending ships against cruise missile attack. We also considered system issues and investigated the limiting factors

that lie beyond the advance technologies considered here. There were several topics that emerged as being of special interest, namely:

- Dynamic range: How much is needed and how to get it?
- Processing and interpretation of phased array data: What is the best processing scheme?
- Direct digital synthesis of signals as an alternative to true time delay beam steering.
- How does one best exploit the new technologies becoming available?

2 AIR DEFENSE CONSIDERATIONS FOR SHIPS

As discussed above the primary cruise missile threat to Navy ships is the sea skimming, Exocet type, missile. As missile radar cross sections are reduced, higher speed missiles are used and multiple guidance and homing techniques, as well as coordinated attacks and penetration aids, are employed defense becomes increasingly difficult. An advanced airborne radar that would perform the detection, tracking and illumination roles out to ranges of about 200 nm is probably the greatest single defensive asset to counter current and advanced cruise missiles. Requirements for such a radar can be summarized by the following time sequence of steps:

1. Detection of target at extended range ($\sim$ 200 nm).
2. Identification of target as a threat.
3. Target tracking.
4. Standard missile (SM-2) launch.
5. Target tracking for command control guidance of SM-2.
6. Illuminator lock with backward looking SM-2 sensor.
7. Illumination of target for semiactive homing of SM-2.
8. Kill assessment and retargeting if necessary and possible.

The detection and tracking problems are hard because the target has such a small radar cross section compared to ocean clutter and the time available to perform the defense system functions is so short. Only thirty to ninety seconds are available for action if the detection horizon is the 15 nm

provided by a mast top radar. An airborne radar with 200 nm range allows a shoot-look-shoot capability and more time to distinguish friend from foe. This summarizes the challenge of an advanced airborne radar for ship defense and provides the focus for the technology research supported by this ACI. ACI technologies should be assessed against this challenge.

In the detection and identification phase (items 1 and 2 above) a very small radar cross section (RCS) target must be detected against a background clutter echo power some 10^9 to 10^{12} times larger. The trick is to use Doppler processing so that a very rapidly moving target can be separated from the very slow moving ocean clutter. The magnitude of the problem can be assessed by comparing a typical target echo with a variety of likely clutter echoes. To quantify the problem we made such a calculation for an X-band radar.

The standard radar equation, e.g. as given by Kingsley & Quegan (1992), yields the received, echo power from a target, P_{tg} as

$$P_{tg} = \frac{P_t G_t G_r \sigma_{tg} \lambda^2}{(4\pi)^3 R^4} \tag{2-1}$$

where P_t is transmit peak power, G_t is transmit antenna gain, G_r is receiver antenna gain, σ_{tg} is target radar cross section, λ is radar wavelength and R is radar range. The expression for clutter power P_c is similar to Equation (2-1) except that the σ is given by the normalized radar cross section of the Earth's surface (σ_c°) multiplied by the surface area within the radar's resolution cell on the surface, i.e.

$$\sigma_c \rightarrow \sigma_c^\circ A_{ill} = \sigma_c^\circ \frac{\Theta_H R \delta R}{\cos \alpha} \tag{2-2}$$

where Θ_H is the horizontal antenna beamwidth, δR is range resolution ($c/2B$), B is radar bandwidth and α is grazing angle. This expression is only valid for small values of α since the vertical antenna beam width limits σ_c at large values of α. Using the analog of Equation (2-1) with Equation (2-2) the

target-to-clutter ratio becomes

$$R_{tc} \approx \left(\frac{\sigma_{tg}}{\sigma_c^\circ}\right)\left(\frac{2B\cos\alpha}{\Theta_H Rc}\right) . \tag{2-3}$$

For an antenna of 1 meter horizontal dimension, a wavelength of 3 cm, a radar bandwidth B and a grazing angle of $\sim 10°$ the target to clutter power ratio becomes

$$R_{tc} \approx 2 \times 10^{-7}\left(\frac{\sigma_{tg}B}{\sigma_c^\circ R}\right) . \tag{2-4}$$

Examples of the results of Equations (2-3) and (2-4) are given in Figures 2-1 and 2-2. Figure 2-1 illustrates the dramatic changes in target to clutter ratio as target and clutter parameters change as well as the relatively weak dependence of R_{tc} on range. In Figure 2-2 we see how radar bandwidth impacts R_{tc} through the size of the range resolution cell.

To summarize consider this example. At a range of 200 nm with typical ocean clutter (normalized radar cross section, $\sigma_c^\circ = 10^{-3}$) and a very low RCS target the target-to-clutter ratio would be ≈ -60 dB. The $\sigma_c^\circ = 10^{-3}$ number is an average σ_c° for X-band sea clutter at low grazing angles ($< 25°$) taken from Wetzel (1990). A signal to noise ratio of 15 dB gives high probability of detection (> 0.999 per pulse) with a low false alarm rate ($< 10^{-6}$). Thus, a Doppler radar with a dynamic range of roughly 75 dB would be sufficient for detecting cruise missiles in this situation. Over typical land the clutter power is greater ($\sigma_c^\circ \sim 10^{-2}$) and ≈ 85 dB dynamic range would be required, again for a very low cross section target. If we consider a situation with very nasty land clutter ($\sigma_c^\circ = 1$) and a very, very low RCS target, the required dynamic range becomes 115 dB. So we conclude that while a dynamic range of 75 dB would handle a typical ocean situation, a goal of 120 dB dynamic range is commensurate with detection and tracking of very, very low RCS targets in very nasty land clutter at ranges of 200 nm. The target to clutter ratio increases as range decreases and so the required dynamic range decreases by about 3 dB at 100 nm and by about 10 dB at 25 nm. Clearly the requirement

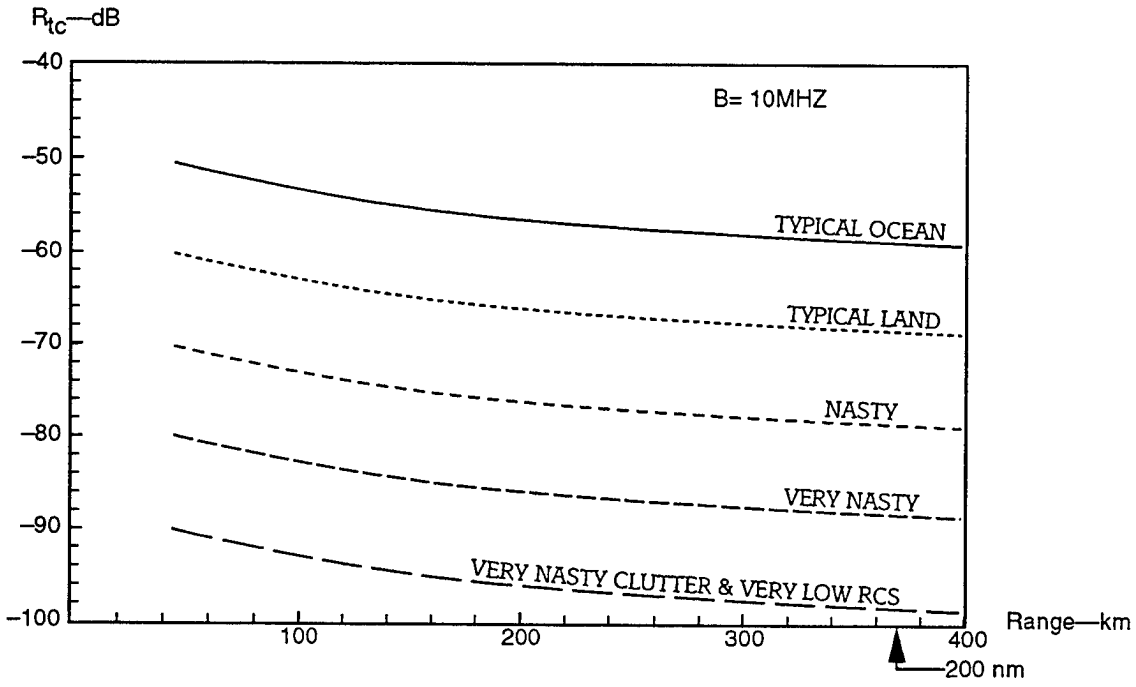

Figure 2-1. Target to clutter ratio for varying range with a variety of target and clutter parameters. The top four curves use a low value of σ_{tg} and the lowest curve uses a very low value.

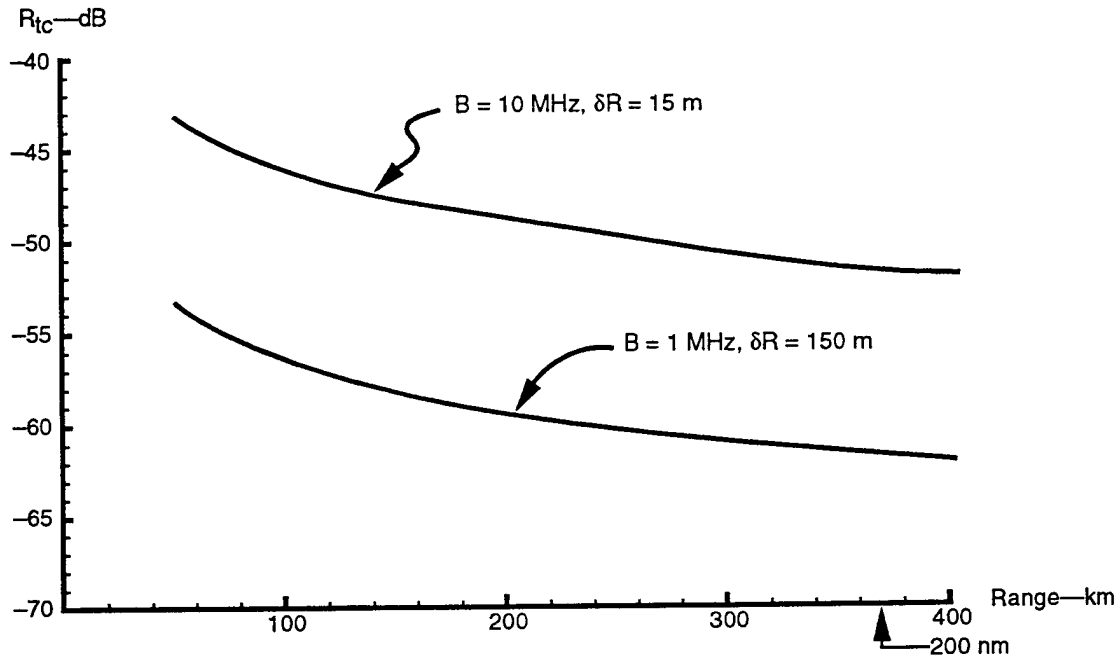

Figure 2-2. Target to clutter ratio for varying range. Note the effect of an increase in bandwidth

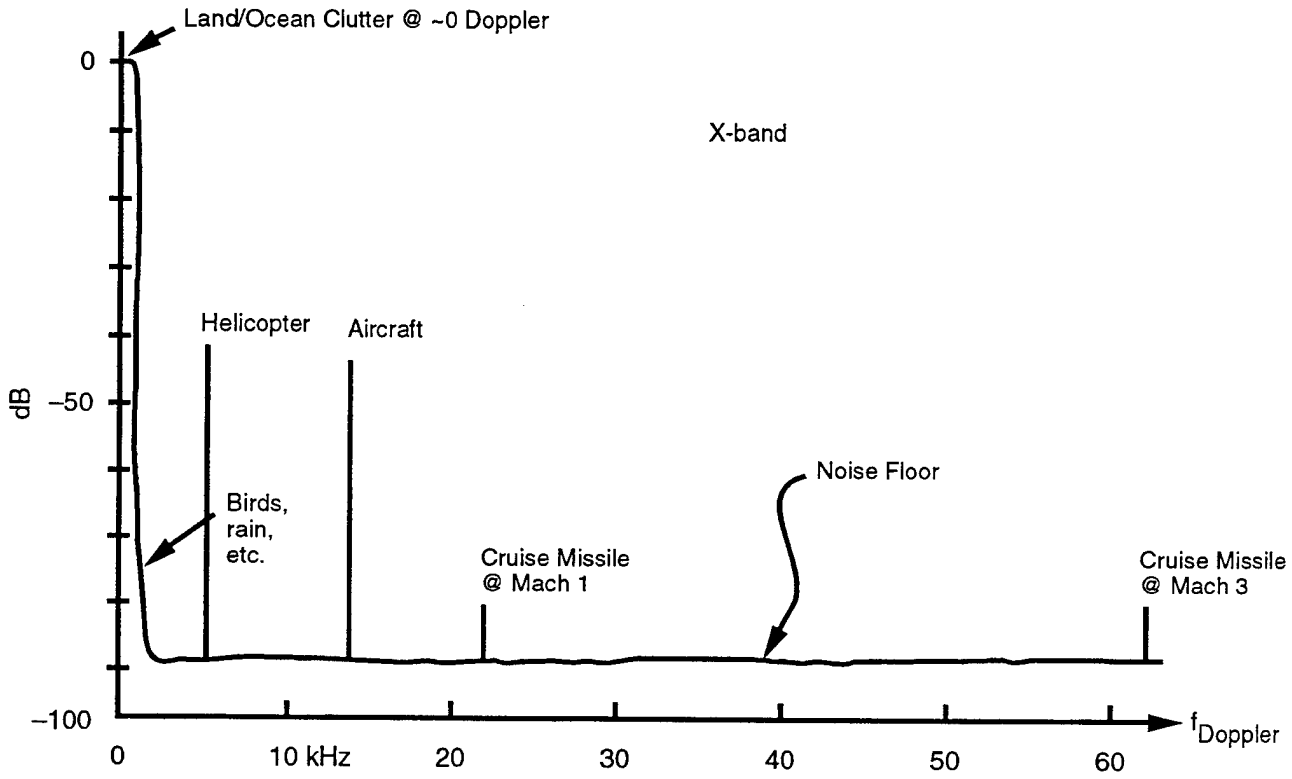

Figure 2-3. Approximate schematic diagram of Doppler spectrum with targets and clutter of various types. We show only the spectrum for positive (approaching) Doppler shifts. There is, of course, a negative (receeding) Doppler specrum as well.

to detect and track over land is realistic since the Persian Gulf, for example, is typically only a little over 100 nm wide. The calculations done here are order of magnitude and we recommend a more detailed system study to determine the dynamic range requirement for anticipated situations.

The very small target to clutter ratio in Figures 2-1 and 2-2 illustrates clearly that Doppler processing is necessary to distinguish targets from the clutter background. Doppler processing separates the land/ocean surface clutter that is near zero Doppler, from moving targets, such as helicopters, fixed wing aircraft and cruise missles. An idealized Doppler display is given in Figure 2-3 with various targets shown according to their expected Dopper shift for direct (radial) approach to the radar. We have shown the noise floor at -90 dB below the clutter as a 'typical' case for an advanced radar. The -90 dB is determined primarily by analog to digital conversion (ADC) speed and dynamic range. As we point out below, the ultimate physical limit to which this noise floor can be pushed is unknown. Ocean surface and radar scattering processes, such as breaking waves and multiple scattering, may be involved. Since the Doppler background required for detecting very low RCS targets may be controlled by such processes, they should be investigated as recommended in Section 6.

High velocity targets at X-band have large Doppler shifts and a pulse-Doppler radar must sample the echo signal at a rate that is at least twice the highest expected Doppler shift. For a Mach 1 target, the sample rate (pulse repetition frequency) would need to be about 40 kHz. Such a high rate introduces a serious problem in that the 'unambiguous range' of ≈ 2 nm is much less than the 200 nm range desired. Thus, targets at ranges greater than 2 nm would be at 'ambiguous ranges' and special techniques, such as prf hopping, would be needed to resolve such ambiguities.

Dynamic range issues deserve some additional comment. If one requires 120 dB of dynamic range from a Doppler processor, then 20 bit resolution is required for the input signal. However, as we shall discuss at various points below, there are a number of ways to obtain the 20 bit range needed. Clearly it is advisable to perform range compression before doing Doppler processing so that one can range gate and discard localized regions of extremely high clutter, e.g. mountains. Such range compression might well be done with an analog surface acoustic wave (SAW) device. Although a sacrifice in range resolution, for a given signal bandwidth, would be required, there is no need for very high range resolution and the sacrifice would be modest. One option would be to do partial range compression with very low far range sidelobes, edit out ranges with extremely high clutter; then do further range compression to improve signal to noise and signal to clutter.

The current state of the art in analog to digital converters (ADC's) is about 16 bit accuracy in a 10 MHz band which would imply a 96 dB dynamic range at the output of a Doppler processor. To obtain 120 dB dynamic range at the Doppler processor output one needs 20 bit accuracy at the input. For a single ADC this is indeed a grand challenge. However, as we shall discuss in Section 3, dynamic range can be accomplished by the use of many relatively low dynamic range processors at each antenna element. This distributes the computation load and with a hundred element array the requirement is only about 13 to 14 bits dynamic range on the digital signal coming from each individual array element.

3 A NEW LOOK AT PHASED ARRAY ANTENNAS

3.1 Introduction and Overview

We took a new look at phased array antennas from two perspectives, theoretical optimization and practical implementation. In the theoretical study (Section 3.2 below) we considered the broad question of how to process the signals at the array elements in order to optimize the beamforming capability of the array. In the practical implementation (Section 3.3) we considered a direct digital synthesis approach (called HICAPOR) with the signal at each array element being tailor-made right at the element. In this Section (3.1) we give a brief overview of these two topics with more detailed discussions following in Sections 3.2 and 3.3.

Theoretical optimization. We consider the simple case of a one-dimensional array with array elements spaced at integer multiples of a spacing d. Our primary concern is with the received signal – extensions are made to the transmitted signal where appropriate. A plane wave arriving at an angle ϕ generates a signal $X(t - kd\sin\phi)$ where k is an integer index. If we introduce a time delay kd sin θ at each element and sum we have

$$\sum_{k=1}^{N} X(t - kd\sin\phi + kd\sin\theta) \qquad (3\text{-}1)$$

When $\phi = \theta$, the sum is coherent at all frequencies and the power gain is N^2, corresponding to the N elements in the array. This exercise illustrates 'true time delay' or TTD beam steering on both receive and transmit. Coherence at all frequencies is the great advantage of TTD beam steering as compared

to conventional phase shift steering illustrated by the sum

$$\sum_{k=1}^{N} \lambda_k X(t - kd \sin \phi) \tag{3-2}$$

where the λ_k's are complex multipliers. The λ_k's can be adjusted so that the sum of Equation (3-2) is coherent, but this only works for one ω when we take $X(t)$ of time harmonic form $e^{i\omega t}$. A 'squint' or distortion occurs at other ω.

For phase shift beam steering there are well known techniques for adaptive beam forming and some established indicators of performance, such as beam directivity and side lobe level. However, all of these performance measures are for narrow band operation. How are we to assess the performance of broad band beam forming techniques, such as TTD? We proceed by developing a broad band performance measure that assesses performance, one frequency at a time and then 'averages' in a rough sense over all relevant frequencies.

In comparing TTD with phase shift steering we find the big advantage for TTD is wide band steering of a single beam without the squint distortion of phase shift steering. However, we also find some disadvantages of the TTD technique. As illustrated in Equations (3-1) and (3-2), TTD allows N degrees of freedom in array steering while 'phase shift' method allows 2N via the complex multiplication by the λ's. The fewer degrees of freedom and the placement of the control as a time delay mean that it is relatively difficult to do adaptive forming of multiple beams by TTD alone. Clearly flexible steering of multiple beams can be done using TTD, but requires different techniques, not yet perfected. A further difficulty of TTD is that for steering much off broad side one needs delays of the order of several to several tens of nanoseconds and a great number of them if there are many sensors in the array. Sophisticated adaptive beam forming for multiple beams will almost certainly be a key requirement for an advanced ship defense radar.

In microwave radars, hybrid systems using both time delay and phase shifters have been used for some time. This appears to be a fruitful approach.

We have worked out a general theory of signal detection and estimation for broad band array processing based on a stochastic signal model and using directivity as the basic measure of performance. This theory suggests that a hybrid array design, consisting of both phase shifting (λ_k) and time delays ($kd \sin\theta$) – effectively this amounts to tapped delay lines in each sensor – would be a useful construction for broad band processing as mentioned above. Using this theory we find that a broad band antenna tries to optimize itself for a particular beam forming assignment by becoming as nearly as possible a narrow band array. In other words the array finds broad band operation 'unnatural' and attempts within its constraints to behave as a narrow band processor. Further discussion is given in Section 3.2 below.

Direct digital synthesis approach (HICAPOR). The essence of this approach is to synthesize the transmitted signal at each array element (under digital fiber optic control) rather than using delay devices to modify a common signal at the RF carrier frequency. To illustrate this idea we did a strawman design of a High Capability Opto-Electronic Radar (HICAPOR). In this design we provided for 2 transmit beams and N receive beams in an N element one-dimensional array. The transmit waveform is synthesized at each element and the received signal is digitized at each antenna element. Optical fiber is not used to perform true time delay (TTD) steering, but is used to distribute the RF clock and synchronization signals as well as carrying the transmit command digital signal from the radar to each antenna element and bringing the digitized receive signal from each antenna element to the radar signal processor. On transmit the D/A waveform generator at each element is used for both pulse-forming and beam-forming.

The HICAPOR system architecture is illustrated in Figure 3-1. Each array module performs the task of waveform synthesis at the RF frequency of the radar. The key elements in the array modules (right side of Figure 3-1) are as follows:

- Antenna radiating element
- Transmit/receive switch
- Analog to digital converter (ADC)
- Waveform generator.

In transmit mode the waveform generator receives RF carrier and synchronization signals over an analog fiber optic link as shown in Figure 3-2. The information for pulse waveform synthesis arrives over a digital fiber optic link. However, the transmit signal itself is synthesized right in the array module.

The operation of the waveform generator is keyed to the two shift registers that contains the waveform information. The lower (very large) register contains all the information for a complete pulse and is used to load the small, upper shift register. The upper shift register is used to set all the PIN diode switches at one instant of time. As the upper register empties to set the PIN switches, it is reloaded with the information for the switch settings for the next instant of time.

The waveform itself is formed by addition of vector components, formed by phase shifting the carrier waveform by eight different amounts and adding selected elements from this set of vectors. One could use more than eight shifts if greater accuracy is desired. This scheme allows (within limits) assembly of any desired waveform with any desired phase shift or time delay. Thus, the scheme could be used to implement simple beam steering without

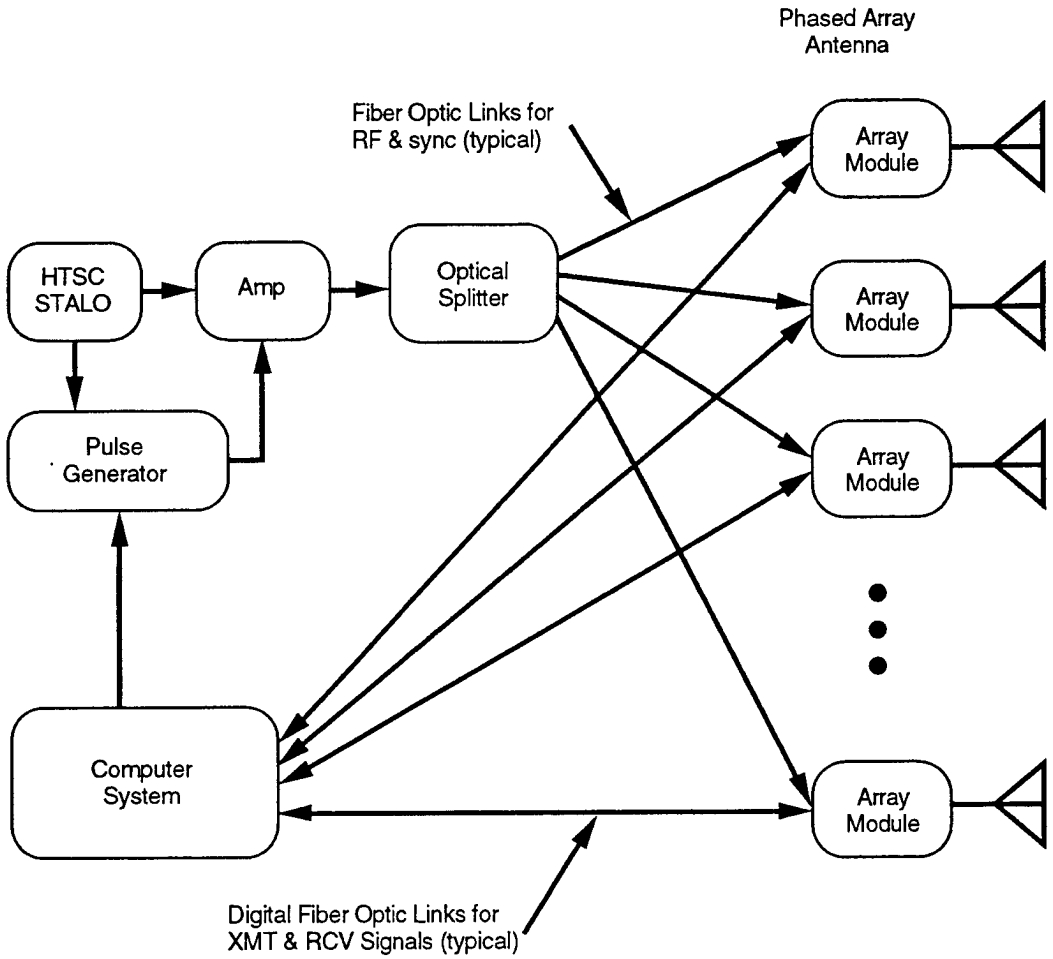

Figure 3-1. Architecture for HICAPOR, High Capability Opto-Electronic Radar. Note that fiber optics are used for signal and control transmission, but not for beam forming. Note also the use of an high temperature superconducting (HTSC) stable local oscillator (STALO).

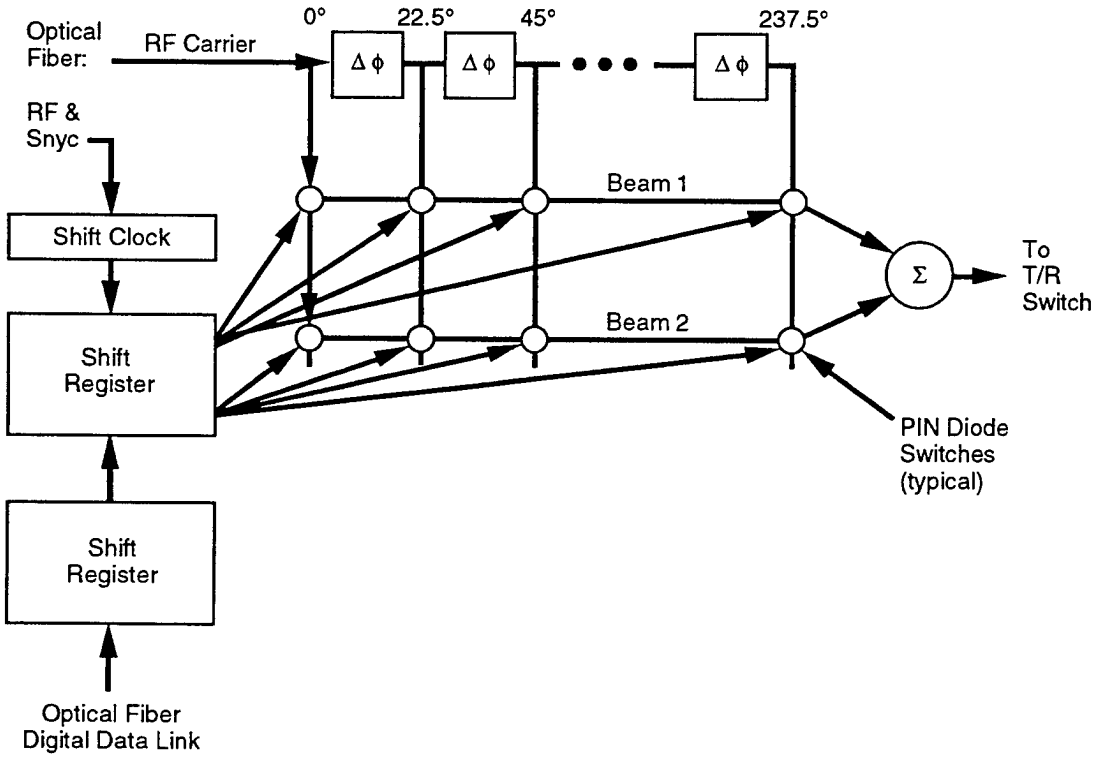

Figure 3-2. Direct digital synthesis (DDS) waveform generator using optical fiber for communications, RF carrier and Sync, but not for time delay.

squint as well as adaptive formation of multiple beams. The case for two beams is shown in Figure 3-2.

On receive, ADC's within the array modules (shown in Figure 3-1) digitize the received signal with a dynamic range of say 13 or 14 bits. This is not the 20 bit dynamic range that is needed to achieve the needed Doppler dynamic range of about 120 dB. However, remember that there are many antenna elements, probably 1000 or more. When we add the contributions of these 1000 elements together the total dynamic range is 13 bits from each ADC plus another 5 to 10 bits from the 1000 additions, depending on noise statistics. A more detailed discussion of HICAPOR is given in Section 3.3.

3.2 Signal Detection and Estimation for Broadband Array Processing

It is not photonically controlled arrays we want to talk about so much as the popular idea they have spawned — that of 'true time delay' steering of radar arrays.

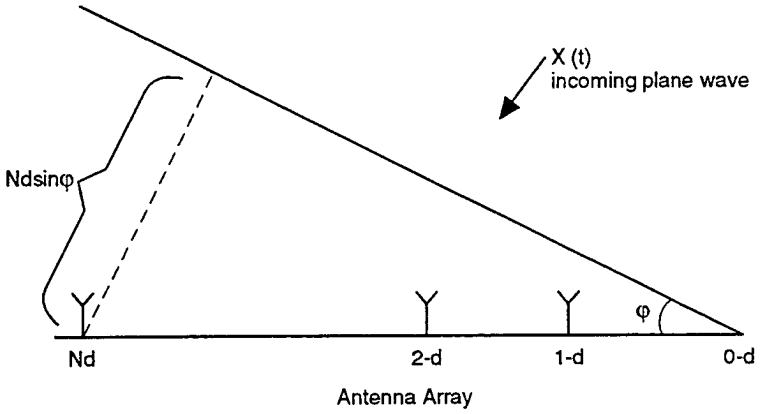

Figure 3-3. Schematic diagram of a phased array antenna with N+1 elements, spaced at a distance d. Also shown is an incoming electromagnetic plane wave.

We take the input at the k^{th} sensor to be $X(t - kd\sin\phi)$. We now time "delay" by $kd\sin\theta$ and sum over k to get

$$\sum_{k=1}^{N} X(t - kd\sin\phi + kd\sin\theta) \; .$$

The above sum is coherent at all frequencies when $\theta = \phi$, and the gain is N^2. The zeroth element is the phase reference for the other elements and so is not included in the sum.

The coherence of the sum at all frequencies is the *great advantage* of true time delay steering, as opposed to phase shift or phase modulation steering in which one forms $\sum_{k=1}^{N} \lambda_k X(t - kd\sin\phi)$. The complex λ_k's can be adjusted so that the sum is coherent for monochromatic X, when $\theta = \phi$, $X(t) = e^{i\omega t}$, $\lambda_k = e^{i\omega kd\sin\theta}$, but there is a "squint" or distortion of the sum at other frequencies. Other λ's give a coherent sum also, for example $\lambda_k = p_k e^{i\omega kd\sin\theta}$, p_k real positive.

Phase shift steering has a number of well known features. For example, there are a large variety of conventional measures of the quality of a phase shift steered array, such as

1. beam width and gain
2. beam efficiency
3. beam directivity
4. side lobe level
5. half power beamwidth

etc., all of which are useful indicators of performance.

In addition, there are well known techniques for steering nulls to desired locations in order to eliminate unwanted signals or compromise jammers. Beyond this, there are a number of adaptive schemes for modifying the λ's to eliminate as much as possible a noisy operating environment. The adaptive schemes effectively try to steer nulls in directions where there is considerable noise power, even when the directions are not known in advance.

All of these "advanced" measures and techniques are for narrow band operation. How are we to measure the quality of broadband beamformers, such as true time delay steering, and how are we to modify the delays in order to steer nulls or eliminate undesired background noise?

A broadband beam former may be considered as operating individually and independently at each of a large number of frequencies, or it may be considered as responding to broadband received signals. If the situation is the former, performance is measured one frequency at a time, and may vary widely with change of frequency. We are interested particularly in the second version. One comes quickly to the realization that many if not all of the usual measures of beam performance are meaningless, though one may look at each of them as operating one frequency at a time. Some reasonable and justifiable method of averaging over all frequencies might fill the gap, and roughly speaking, that is how we are about to proceed.

We first want to argue that pure time delay steering, while it forms a beam with good gain at all frequencies does not readily admit much tuning to meet special circumstances, which may arise quite frequently, such as jamming. We can give an approximate idea of the problems by considering the response of a pure time delayed beam former to an incoming pulse (formed by a jammer say), arriving broadside. Say the pulse width is comparable to the time delay per sensor. Then all we can do with time delays is spread N copies of the pulse around the bearing semicircle, and these not too far

from broadside, unless very long delays are available. This suggests another problem with true time delay steering. For steering much off broadside, one needs long delays; at the very least one needs a great number of delays if there are many sensors in the array. Furthermore, array design is inefficient at low frequencies; since the array element spacing is determined by the highest operating frequency, there are enough additional array elements at low frequencies for sophisticated beam forming at these frequencies.

In phase shift steering there are $2N$ degrees of freedom by the choice of complex phase modulations. The true time delay steering has only N degrees of freedom, (i.e. the N times delays). From the point of view of analysis, the N degrees of freedom are awkwardly placed — it is simply difficult to see how to modify the delays to get desired results, other than the one result which is their claim to prominence.

In the appendix to this report a general theory of signal detection and estimation for broadband array processing is worked out. This theory suggests that a hybrid array design, consisting of both phase shifting and time delays — effectively this amounts to tapped delay lines in each sensor — might be a useful construction for broadband processing. A useful modification might be a single phase shift and variable delay per sensor. The truth of the matter is that broadband processing was shoe-horned with some difficulty into this hybrid design, but the design does afford potentially the advantages of both types of array processing, and is worth analyzing in its own right. The design has the additional great advantage of easy analytic manipulability.

We will illustrate some of these features now. It was a feature of the general theory, and it is essential for the analysis now that the signal source be described stochastically, so arriving signals will be taken as sample paths from a stationary stochastic process, with known covariance and power spec-

trum. It is the known power spectrum which gives us the chance to average performance per frequency over frequency, though as an expression of our ignorance we often take flat power spectrum over frequency ranges of interest.

We denote the covariance by $R(\tau)$ and the power spectrum by $S(\omega)$. R and S are a Fourier Transform pair.

The measure of beam quality that we intend to use is derived from the familiar notion of beam directivity, but we must replace it by stochastic beam directivity. Directivity has been in the past a commonly used device for beam forming, though it has its limitations and has occasionally led to over design.

We take for a first example N sensors in a linear array, each with a simple delay, Δ, available, or no delay. Thus if the sensor receives $f(t)$, it can replace it, for processing, by $\lambda f(t) + \eta f(t - \Delta)$.

Suppose a signal $X(t)$ is arriving broadside. Our array of N sensors could construct

$$\sum_{k=1}^{N} \{\lambda_k X(t) + \eta_k X(t - \Delta)\} .$$

For the signal $X(t)$ arriving from angle ϕ, the same array will construct

$$F_\phi(t) = \sum_{k=1}^{N} \lambda_k X(t - kd \sin\phi) + \eta_k X(t - kd \sin\phi - \Delta) .$$

The expected value of $|F_\phi(t)|^2$ is

$$\sum_{k,\ell=1}^{N} \Big\{ \lambda_k \bar{\lambda}_\ell R((k-\ell)d \sin\phi)$$

$$+\lambda_k \bar{\eta}_\ell R((k-\ell)d \sin\phi - \Delta)$$

$$+\eta_\ell \bar{\lambda}_k R((l-k)d \sin\phi + \Delta)$$

$$+\eta_k\bar{\eta}_\ell R((k-\ell)d\sin\phi)\}$$

since the expected value of $X(t+a)\bar{X}(t+b)$ is $R(b-a)$.

The expectation, call it $E(\phi)$, is thus an Hermitian form in the complex variables λ and η. By analogy with the conventional definition of directivity, we define the stochastic directivity for broadside steering as

$$\frac{E(0)}{\int_{-\frac{\pi}{2}}^{\frac{\pi}{2}} E(\phi)\cos\phi d\phi}.$$

We construct a beam with best broadside directivity by holding $E(0)$ fixed at one, and minimizing $\int_{-\frac{\pi}{2}}^{\frac{\pi}{2}} E(\phi)\cos\phi d\phi$.

This is just the minimization of one semi-definite Hermitian form with another form held fixed, and is readily solved computationally. If the signal is broadband, the form $\int_{-\frac{\pi}{2}}^{\frac{\pi}{2}} E(\phi)\cos\phi d\phi$ is positive definite.

There are, of course, analogous formulations for best directivity steering in other directions as well. Notationally, the situation becomes more complicated as the number of delays per sensor increases, though the final problem is always the same one of minimizing one form, holding another fixed.

The simplest treatment perhaps, at least notationally, is to go to the continuum limit and let each sensor apply an arbitrary linear filter to the received signal, even a non-causal filter. So for a broadside incoming signal $X(t)$ the array sees at the k sensor in the look direction ϕ the quantity

$$U_k(\tau) = \int_{-\infty}^{\infty} L_k(\tau - t)X(t - kd\sin\phi)dt$$

and the array processor forms $F_\phi(t) = \sum_{k=1}^{N} U_k(\tau)$. The expected value of $|F_\phi(t)|^2$ is then $E(\phi)$

$$\sum_{k,\ell=1}^{N} \int_{-\infty}^{\infty}\int_{-\infty}^{\infty} L_k(t)\overline{L_\ell(s)}R(s-t+(k-\ell)d\sin\phi)dsdt$$

from which the formulae for discrete delays follows easily by putting L_k equal to a weighted sum of delta functions. Letting $\hat{L}_k$ be the Fourier transform of L_k, the above can be thrown into the interesting form (up to simple scale change):

$$\sum_{k,\ell=1}^{N} \int_{-\infty}^{\infty} \hat{L}_k(\omega)\overline{\hat{L}_\ell\omega}\, e^{i\omega(k-\ell)d\sin\phi} S(\omega)d\omega$$

with S the power spectrum. The average over ϕ may be performed to yield

$$\int_{-\frac{\pi}{2}}^{\frac{\pi}{2}} E(\phi)\cos\phi d\phi$$

as

$$\sum_{k,\ell=1}^{N} \int_{-\infty}^{\infty} \hat{L}_k(\omega)\overline{\hat{L}_\ell(\omega)}\, \frac{2\sin(k-\ell)d\omega}{(k-\ell)d\omega} S(\omega)d\omega\ .$$

Notice that the above expression, which is to be minimized subject to constraint, is just the average, weighted by the power spectrum, of individual frequency performance measures. The constraint is:

$$\int_{-\infty}^{\infty} |\sum_{k=1}^{N} \hat{L}_k(\omega)|^2 S(\omega)d\omega = 1\ .$$

Displayed in this form the minimization problem is basically uncoupled by frequency, and can be solved "explicitly" though the optimal solution is not an attained one. Let $D(\omega)$ be the ordinary directivity of this array at frequency ω — by ordinary here we mean with one phase modulation per sensor, and let $\mathcal{S}$ be the set of frequencies in the support of $S(\omega)$ at which $D(\omega)$ takes its maximum value. Then the L_k's are pass filters, passing only the frequencies in $\mathcal{S}$, each pass frequency modulated by complex numbers scaling like those which gave rise to the optimum solution $D(\omega)$. In other words the array is behaving like a modulated pass for special frequencies only. This result is a little disappointing but somewhat revealing — broadband beam forming for special purposes is going to be unnatural — the array will try to behave like a narrow band processor.

Of course, having the delay lines and modulating constants available will give a better beam for special purposes than simple true time delay steering.

One could even try a minimum variance distortionless beam forming also, if noise statistics are available. Given the large number of tunable variables present in the array, it might be best to estimate several consecutive signal values at once, minimizing their total variance, and keep a shifting record of the estimates as the process advances in time.

3.3 A Strawman High-Capability Opto-Electronic Radar (HICAPOR)

3.3.1 Introduction

It is clear from the above discussion that new developments in opto-electronics will certainly impact new radar systems. This impact will vary with the type of radar; its application, performance, operating modes, beam types and transmitted waveforms. For example, it appears that the use of opto-electronic time-delay systems can greatly improve simple 'phased-array' radar systems with a single transmitted beam of simple waveform and a simple signal beamforming for the received signal. In this section we will propose a new approach for highly flexible, high-capability, 'phased-array', radars that make use of the best of, not only current (and developing) opto-electronic technology, but the best of computer technology as well. It is designed to provide the maximum flexibility by minimizing fixed hardware, and putting as much configuration capability into software as possible. We call this concept 'HICAPOR' for High Capability Opto-Electronic radar. It is presented here as a 'strawman' concept to stimulate further discussion of

how both opto-electronics and computers can synergistically impact future radar systems.

3.3.2 Requirements

We assume that we will want to have RF radar pulses with carrier frequencies between one and one-hundred GHz. Also we will want to have several simultaneous transmitted beams of different character, such as a scan beam and a tracking beam. Finally we will want to provide for adaptive beam-forming to steer nulls, etc.

3.3.3 Opto-Electronics

Opto-electronics with its solid state lasers, modulators, detectors and optical fiber, offers low cost transmission of very wide-bandwidth, coherent RF signals, control information, and digital data, between the array elements and the other components of the radar. It is possible to coherently distribute (or collect) 90 GHz RF signals and 10 Gbits/sec digital data many meters over a single fiber. While opto-electronics can also be employed for information processing such as beamforming, it can suffer disadvantages of flexibility, etc. relative to digital integrated circuits and digital computers. So we will attempt to employ opto-electronics just where it is most advantageous to do so. This will be in the distribution of a highly coherent RF carrier and the transmission of wideband digital control and data.

3.3.4 Digital Processing

Today digital circuits are limited to speeds of about 40 Gbits/sec in exotic technologies, and about 1 Gbit/sec in CMOS technology. Today's best single-chip CMOS microprocessor (the DEC Alpha) achieves about one Gop/second. Today's COTS (commercial off the shelf) memory chips are limited to 64 Mbits, but laboratory chips achieve 256 Mbits/chip. A small cabinet can hold ten boards, each of which can hold about 1000 chips or about 10,000 chips total. As we will show below, we will use a small amount of exotic integrated circuit technology at each antenna element to help form a transmitted beam (PIN switches and analog T/R modules) and in high-performance A/D (Analog to Digital) converters to sample the received signal in each antenna element.

Receiver beamforming is done by computer. Basic beamforming is mostly coherent addition. A single received pulse on a single antenna element will require, after down-conversion and A/D sampling, about 10,000 words of about 16 bits each to represent the received signal. This will be about 20 Mbytes for a whole antenna of about 1000 elements. This data is easily stored in a few COTS chips. Assuming about 1000 pulses/second, the required computer operations will be 20-100 Gops, also doable in a modest number of COTS chips. The complete processor should easily fit into a single cabinet.

3.4 HICAPOR Architecture

The HICAPOR architecture is illustrated in Figure 3-1 above. It is composed of a very stable RF source, illustrated here as a HTSC (High-Temperature Super Conducting) STALO (Stable Local Oscillator.) It provides, not only the RF source, but also the phase reference for the pulse generator. From the STALO the RF signal is amplified and fed to an optical modulator that modulates the carrier RF into an optical carrier. A separate optical carrier is modulated with a 'start' pulse by the pulse generator. The RF optical signal and the 'start' pulse optical signal are then combined. The optical signal is then split $\sim$ 1000 ways into separate fibers that go to each antenna array module. Careful adjustment of the length of each fiber assures that each module receives each start pulse and RF signal at exactly the same time. The pulse generator also feeds a synchronous clock signal to the computer system.

The computer system has a separate digital optical fiber link to each antenna array module. The computer can load, ahead of each radar pulse, a unique specification for the waveform to be transmitted by each array module. After the 'start' pulse causes each array element to transmit its waveform, the array element switches to receive mode and digitizes the returned signal. About 10,000 samples per array element are then sent to the computer system over the same digital optical fiber link.

3.4.1 Array Module

The array module is shown in Figure 3-4.

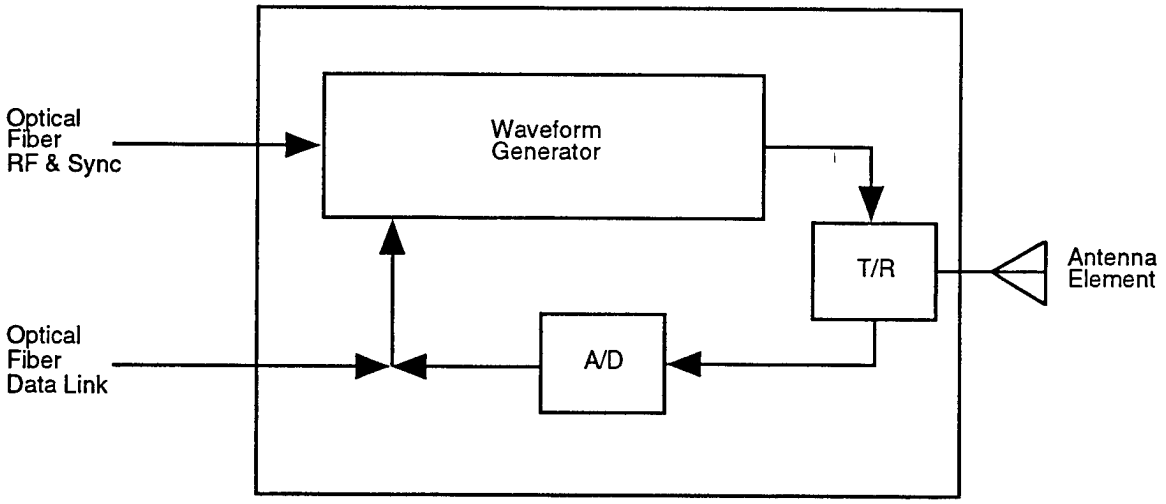

Figure 3-4. Array module.

It has a waveform generator that generates the desired radar RF pulse waveform. The signal is then amplified and switched to the antenna element by the T/R (Transmit/Receive) module. After a small delay, the T/R module switches to receive mode and the A/D (Analog to Digital) converter module digitizes the received signal and formats it for transmission back to the computer system. (An attractive alternative would employ a wide dynamic range analog optical modulator at the array module, with the A/D conversion then performed at the central location of the computer system.)

The conversion rate of the A/D converter depends upon the IF (Intermediate Frequency) bandwidth. If it is possible to directly A/D convert the received signal, there is a big advantage for flexibility. However the state of the art of A/D converters limits the sample rate to about 500 MHz for a precision of 10 bits. (See Figure 3-8). Thus most radar modes will require down conversion to IF or baseband frequencies of bandwidth less than 250 MHz. The down conversion frequency can be supplied by the same optical fiber that carries the RF carrier signal to the array module. After sending the RF carrier frequency to the array module, the frequency generator shifts

to the conversion frequency which switches the T/R module to receive mode and down converts the received radar signal to IF or baseband frequency. Then it is digitized by the A/D converter and transmitted to the computer system.

If the A/D converter has a resolution of 10 bits, then 1000 such elements will add 10 more bits after beamforming to provide about 20 bits of resolution in the received signal after beam forming. Noise properties may modify this situation, requiring more A/D converter resolution; but very significant gains in dynamic range result from the addition of signals from each element.

The waveform generator is shown in Figure 3-2. Transmit beam forming is a combination of amplitude modulation, time delay and phase shifting. Prior to the generation of a transmitted pulse, a waveform specification is sent by the computer, via the optical fiber data link, to the array module. It is bit-serial shifted into the link shift register. The shift register allows the parallel transfer to the waveform shift register, which provides character ouputs (e.g. 8 bits) to the PIN switches. This shifting is controlled by the synchronization pulses distributed over the optical fiber RF and sync link and is coherent with the RF carrier frequency. The carrier frequency itself is sent through a series of transmission lines each of which provides a time delay corresponding to a phase shift of 22.5°. By selecting which PIN switches to turn on and when, a wide variety of transmitted beams can be generated, as shown in Figures 3-5 to 3-7.

3.4.2 Waveform Generation

The basic beamforming method is to provide for each antenna element in the array, a close approximation to the exact waveform needed to form a high quality beam. The computer will calculate for each element, the

gross starting time for each waveform, and the phase of each waveform. The character string representing this information is then transmitted over the optical fiber data link to each element.

Figure 3-5 is an example illustrating the forming of a simple single-pulse beam. First the RF carrier is sent to the module. When the master sync pulse arrives, it begins the shifting of control characters out of the shift register. A string of zeros provides the gross delay as no PIN switches are activated. When the string of character '2' arrives, the proper phase is selected by turning on the corresponding PIN switches. The result is a very close approximation to the correctly delayed and phased waveform. This waveform is then amplified and sent to the antenna element by the T/R module.

Figure 3-6 illustrated how two simultaneous, but independent, beams can be formed. The two sets of PIN switches, as shown in Figure 3-2, are employed. Again the delay, duration and phase for the pulse for each beam is calculated by the computer. The control character streams are combined and sent to the array element. Upon shifting out, the characters activate the PIN switches, and the two waveforms are combined and sent to the T/R module.

Figure 3-7 illustrates how pulse compression is achieved by waveform phase encoding. A suitable pulse-compression code is chosen by the computer system, the desired waveform calculated and a string of control characters appropriate for each element is sent to each array module. Again the PIN switches select the desired phase for each time element.

While creating such a "spread" transmitter pulse is straightforward, the reception of the reflected signal is difficult. It is difficult because now the sampling rate of the A/D converter must be at least twice the rate at which

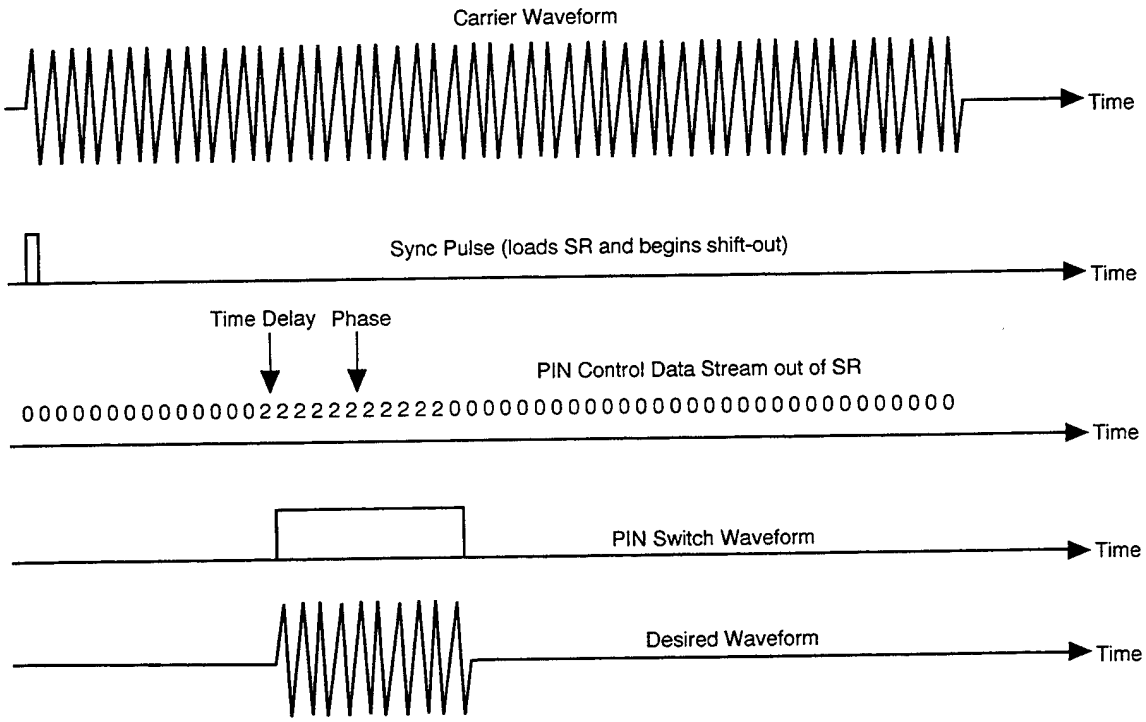

Figure 3-5. Simple pulse waveform.

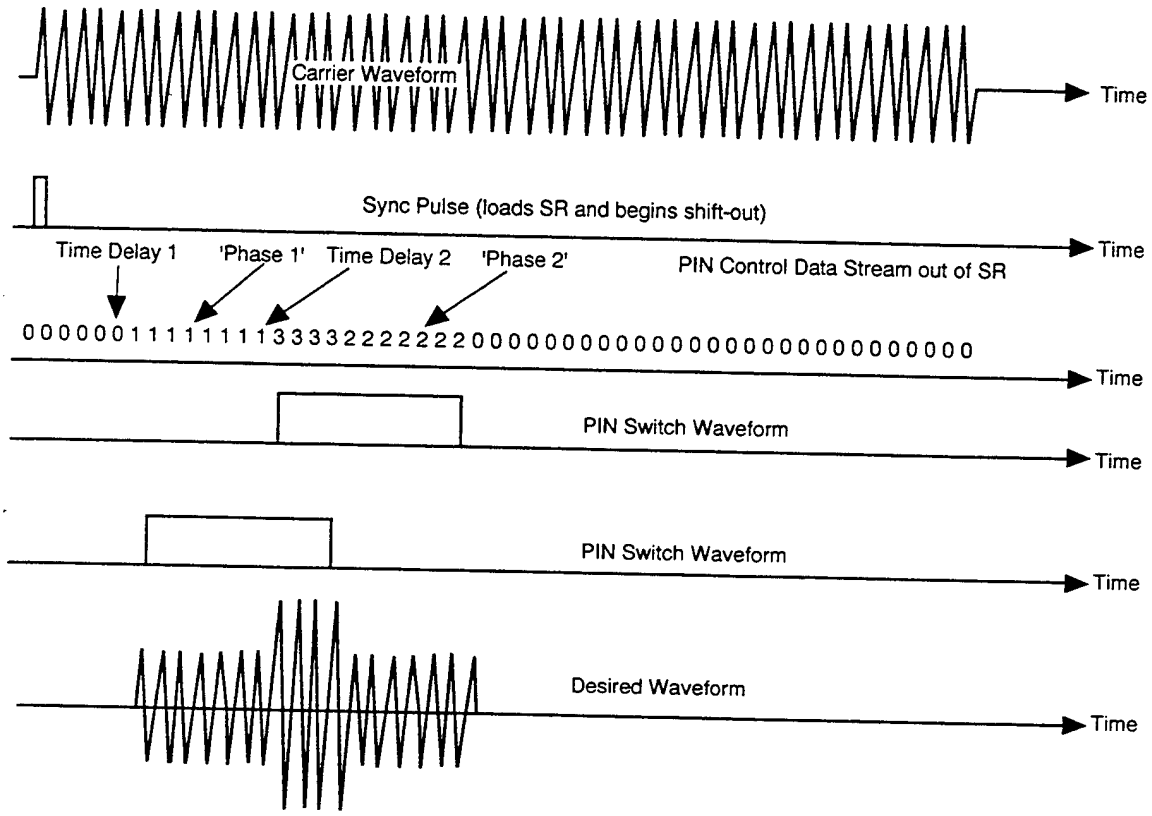

Figure 3-6. Waveform for two beams.

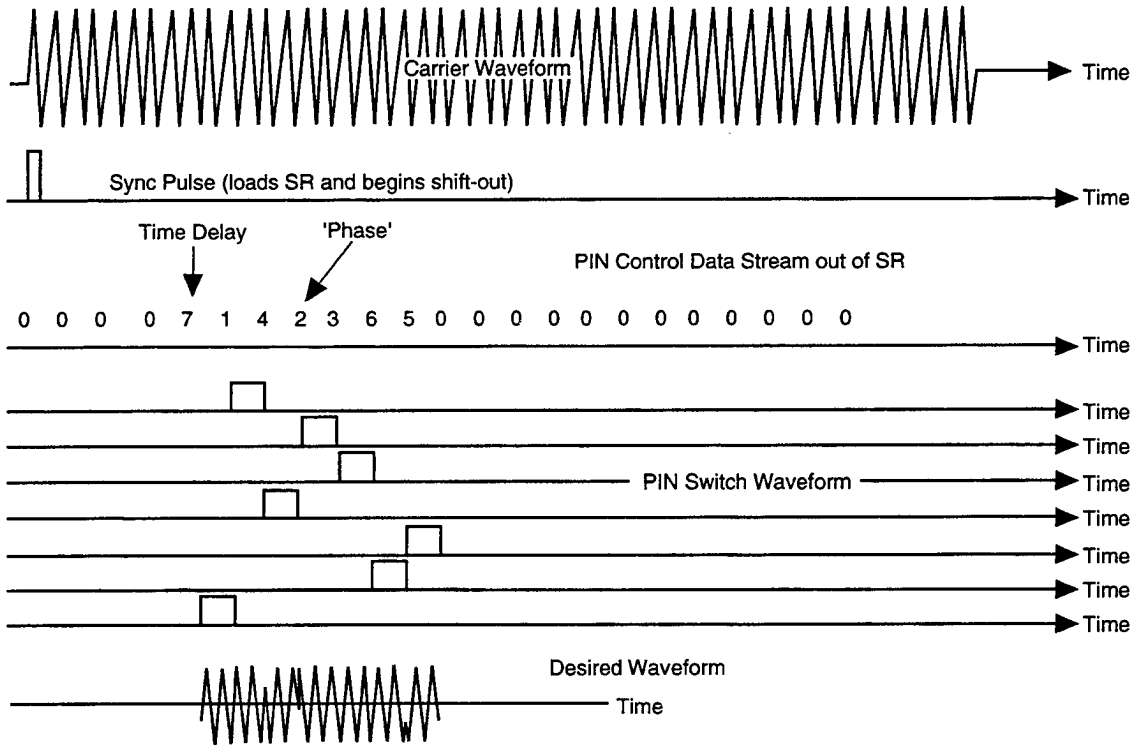

Figure 3-7. Pulse compressed waveform.

the phase of the transmitted waveform changes. Depending upon the exact parameters chosen, sampling rates 100 times larger may be needed. While fewer bits of resolution per sample would be needed, this still is a challenge to state of the art A/D converters. For example if 4 bits per sample are employed, sampling rates are limited by today's A/D converts to about 5 GHz (see Figure 3-8). Future improvements in A/D converters will make this radar operating mode more attractive. Note also that the beamforming computation process must now perform pulse compression summing as well, thus greatly increasing the processing requirements.

To some extent fast multiplexing can be used to run "slow" ADC's in parallel to accomplish a faster sample rate. Thus, one can 'slide' up and down the trend line in Figure 3-8.

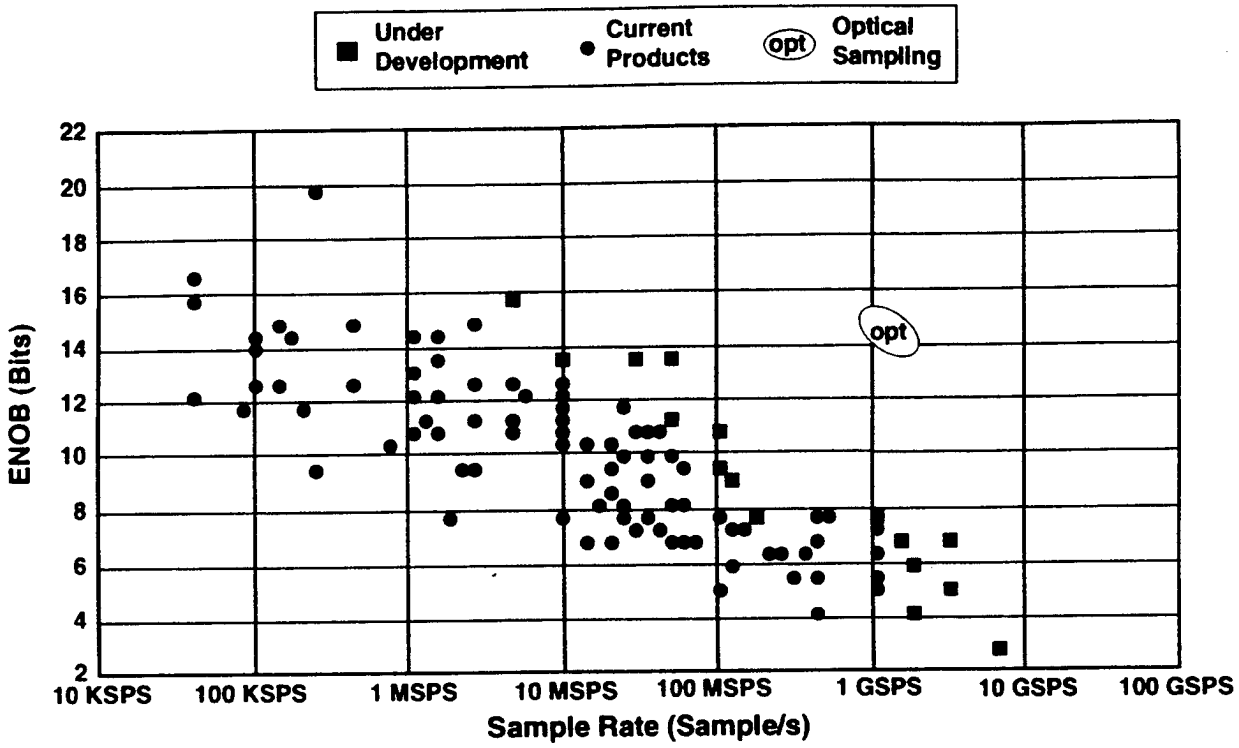

Figure 3-8. Analog to Digital Converter Performance, effective number of bits (ENOB vs. sample rate. (Chart courtesy Lincoln Laboratories, 1997)

3.5 Summary

In summary we see that the HICAPOR system can provide very flexible radar systems by employing computer calculations to determine transmitter pulse characteristics individually at each array element. Each transmitted pulse can be unique, shifting carrier frequency, pulse compression, beam number, beam sizes and beam directions pulse to pulse. Time delay and phase coherence is inexpensively provided by opto-electronics, with a large reduction in the size, weight, power and cost of the antenna phased array over classical designs since the massive maze of microwave plumbing is eliminated. Clearly the HICAPOR design is incomplete, but it should be useful for stimulating new approaches to modern radar design.

4 ASSESSMENT OF ACI TECHNOLOGY INITIATIVES

4.1 Introduction

Three criteria were used in assessing the advanced radar technology discussed below. First, how relevant was the item to the fleet air defense problem discussed above. Second, how likely was the proposed technology to be successfully developed and finally how cost/effective would the implementation of the item be when introduced into advanced radars. Our goal is to point out the most promising technologies as well as some of the potential pitfalls and worries we have concerning these technologies. We considered the following technologies, some only briefly and some in more depth:

1. *Cryo Radar* using High Temperature Superconductor (HTSC) Devices, e.g. ultra stable local oscillators, channelized filters and high dynamic range analog to digital converters (ADC's)
2. *Optics and Photonics*
3. *GEISHA*: Wide Bandgap semiconductor devices for wide bandwidth microwave amplifiers
4. *Ultra Wideband Antennas*

4.2 Cryo Radar

Cryo radar is a 'catch all' phrase to describe a group of high temperature superconductor (HTSC or simply HTS) technologies applicable to advanced microwave radar. HTS materials show superconductor properties at temperatures in excess of the liquid Nitrogen temperature of 77° K and as high as 130° K. For example, HTS techniques have been applied to transmission lines as well as passive and active components, including very high Q resonators. Since an HTS film has a very low resistance, the Q, which is the ratio of energy stored in a resonant circuit to the energy dissipated, can be very high. High Q means a very sharp resonance. A high Q resonator is a device in which a material, such as sapphire, is sandwiched between two HTS films. Such resonators can be used in filters as well as low phase noise oscillators

HTS, ultrastable local oscillators have been demonstrated by a number of workers, e.g. Flory and Taber (1993).[1] These devices demonstrate extremely low phase noise levels out to tens of MHz from the carrier frequency. For example, a level of below -125 dBc/Hz was reported by Shen (1994, p. 231) [3] at 10 kHz offset from the carrier. This level is low enough to allow detection of a very very small target with a radial speed of about Mach 1 if local oscillator phase noise alone were the limiting factor in performance. In fact such a performance level would exceed current performance by 30 dB or more.

The catch here is knowing whether some other factor might be the limiting factor in establishing the clutter/noise floor of a Doppler radar. We point out that other factors may be involved. For example, there may be multiple scattering processes that could produce very low level backscatter echoes at Doppler shifts of tens of kHz in ocean clutter. The levels we are dealing with are extremely low and previously neglected processes may

come into play. To resolve this issue we recommend construction of a simple CW or FM-CW radar using a HTS local oscillator to find out how low the clutter/noise floor really is when observing the real ocean.

Finally we note that HTS low phase noise oscillators are not a 'piece of cake' to build and may have some performance characteristics that need to be dealt with. For example, Shen (1994, Figure 7.9) [3] shows a phase noise spectrum that is 'relatively' clean. Nevertheless, 40 dB spikes in the spectrum of unknown origin were present at frequencies of tens of kHz. Such spikes would need to be eliminated to make such a HTS local oscillator practical for an advanced performance radar.

Another microwave application of HTS films is in the construction of filters with very high out-of-band suppression using a series of coupled sapphire resonators. These devices are capable of handling high power. In advanced radars such devices could be used to suppress out-of-band jammers sufficiently to allow operation of a very high sensitivity Doppler radar as desired here.

We looked briefly at very high performance analog to digital converters (ADC's), such as might be possible using Josephson junctions. One approach to high dynamic range ADC's is the 'sigma/delta' design. The basic scheme is to count pulses (the deltas) until the sum of these (the sigma) is equal to the incoming signal. For small amplitude pulses this scheme works well. However, the sigma/delta scheme is vulnerable to slope overload, i.e. a sharp edge in the signal time series becomes a linear slope if the change in level is large. For example, a square pulse could become a triangle pulse if the pulse amplitude is large enough. The problem for a radar is that the sigma/delta scheme fails just when you need it most – in a high level clutter situation.

We think that there are ways, other than simply building a 20 bit ADC, to obtain the 20 bit ADC resolution in a 10 MHz bandwidth necessary for a very high performance Doppler radar. One alternative was discussed earlier in connection with the HICAPOR radar design concept (Section 3, above).

4.3 Optics and Photonics

There are a number of advantages of using optical fibers and photonic devices in radar systems. For example, optical fibers are very high bandwidth and resistant to interference by unwanted microwave signals, e.g. RFI and jamming. However, we think that photonics in radar needs to be considered on a system level to find where it makes sense and where it doesn't. For example, we think that it makes good sense to transmit microwave digital control signals and analog signal waveforms from point to point in a radar system via optical fibers. We are less enthusiastic about using photonics to do wideband beamforming, although there are advantages over conventional approaches. Our point is that there are other alternatives beside photonic devices to accomplish wideband beamforming. One alternative is discussed above in the HICAPOR design concept (Section above). Further discussion of the advantages and disadvantages of 'true time delay' beamforming is given above in Section 3.2 .

It is also useful to note some of the fundamental aspects of photonic transmission of microwave signals – analog or digital. The principal advantages of photonic transmission are low transmission loss over large distances (but relatively high insertion loss), very broad bandwidth in a microwave sense, light weight, high rejection of interference and jamming and potentially low cost (but currently rather high at $\approx$ \$5,000 per device). Both direct and external modulation can be used to impress microwave modula-

tion on an optical carrier. To access the relative effectiveness of an optical versus a microwave link one needs to compare the signal to noise ratios in each case. For a microwave link the noise level is set by thermal noise kTB where k is Boltzmann's constant, T is noise temperature and B is the bandwidth of the link to overcome noise. For an optical link the noise level is set by photon shot noise $2h\nu B$ where ν is the optical frequency and h Planck's constant. Thus, for typical conditions (a temperature of 300 °K) about 60 times more power is required in the optical link. Further, the microwave insertion loss of a photonic link is presently from about -10 to -4 dB. These factors stress device and system design in optical analog links because of the high optical power required to obtain high SNR.

Several device issues arose during the JASON Summer Study pointing toward both possibilities for advance as well as possible pitfalls. Directly modulated diode lasers are small and can attain modest power, but are limited to about 10 GHz maximum modulation frequency. Distributed feedback DFB lasers are lower noise than competing Fabre-Perot's. Externally modulated continuous wave solid state lasers are larger and more powerful than the diode lasers and can operate into the mm-wave range. The best dynamic range is attained by combined high power and low noise. Current photodetector response extends to the mm-wave range, but low maximum power limits dynamic range and the scope of photonic fan-in architectures. Performance of both optical modulators (lower $V\pi$, the voltage required to change the optical phase by π radians) and photodetectors (higher power) can be improved by good velocity matching of optical and microwave signals. Coherent detection in an optical system requires very small optical phase shifts in the fiber optics and will probably be difficult to implement robustly outside the laboratory.

4.3.1 Advantages of photonics

Spectacular progress has been made in the field of photonics in recent years, driven by the transition to digital fiber optics in telecommunication networks and by opportunities for fiber optic distribution of analog cable television signals. Using optical fibers it is now possible to transmit optical signals modulated at microwave rates over long distances with little attenuation. The photonic hardware required is typically smaller and much lower in weight than its microwave equivalent. These developments have led to research in the use of photonics for better microwave and millimeter wave systems and radar.

Small size and low weight are important advantages of photonic systems. Because the dimensions of optical fiber are governed by the wavelength of light rather than the wavelength of microwaves, fiber optic cables are inherently small and hence light weight; a kilometer of fiber can be held on a modest sized spool, whereas a kilometer of microwave coaxial cable would be wound on a reel about 3 or 4 feet in diameter, weighing well over a hundred pounds. Photonic sources and detectors are also more compact in many cases than their microwave counterparts.

Optical transmission of microwave signals offers additional advantages. Because the frequency of microwave or mm-wave signals are orders of magnitude smaller than the optical carrier, the properties of the photonic system change little with microwave frequency and the system is inherently broadband. In addition, the optical signal in fibers is practically immune to electromagnetic interference and jamming, creates little or no thermal signature, and is very difficult to detect outside the fiber.

Low cost is often cited as an advantage for photonic microwave systems.

Conventional phased array radars are large, complex, and expensive. Photonic sources and detectors are small and potentially inexpensive; for example the laser diode used in compact disk players cost less than $1. However, photonic devices with the required frequency response and signal to noise ratio for microwave applications are costly (~$5k/device), prohibitively so for complex radars. Amortization of engineering investment and economies of scale could drive prices lower in the future as could the development of integrated optical systems.

4.3.2 Potential applications

Telecommunications has been the primary driver for photonics, because optical fiber is ideally suited to the transmission of high bit rate digital data over long distances. Sophisticated schemes have been developed to transmit, amplify, and manipulate digital photonic signals at high data rates. Early on it was realized that pulses in optical fibers travel as solitons at minima in the attenuation spectra: second order dispersion in the pulse velocity with wavelength acts to keep the pulses temporally sharp. More recently optical amplifiers consisting of erbium doped fibers have been developed to avoid the necessity to detect and retransmit the pulse electronically. These advances are being incorporated into new optical fiber networks.

Phased array radar has attracted much attention as a potential application of photonics, because conventional phased array radars are heavy, complex, and expensive. Photonics promises to reduce radar weight and is particularly suited to light weight conformal arrays for aircraft and mobile ground vehicles. Hughes has recently built and tested a wide band conformal photonic phased array radar demonstration system operating near 1 GHz.

However, the problems of complexity and cost remain, at least for the near future, and must be addressed in research on array architecture.

Applications of mm-waves to radar and electronics are limited by the heavy attenuation of mm-wave signals in conventional waveguides and by the performance of mm-wave devices. Once the frequency of photonic modulators and detectors is increased sufficiently, optical fibers can be used to transmit coherent mm-wave signals over considerable distances. This ability may have important applications in mm-wave system design.

4.3.3 Properties of a Single Photonic Microwave Link

We begin our discussion of photonic radar, by considering the properties of a single photonic microwave link. Two methods of constructing a photonic microwave link are illustrated in Figure 4-1: direct modulation of a diode laser, and external modulation of a solid state laser. Direct modulation is achieved by modulating the electric current through a laser diode at microwave frequencies, thereby modulating the photon current and optical power. Note that the optical power is modulated rather than the optical field, as would be the case for a conventional microwave link. A single mode optical fiber transmits the signal from the source to a photodetector. Photons absorbed in the photodetector recreate the microwave signal by producing an electric current proportional to the optical power. External modulation is similar except the modulated optical signal is obtained by modulating the intensity of a cw solid state laser, using an external modulator, typically a Mach-Zehnder interferometer. In this section we will describe the properties of the photonic devices used to construct both types of microwave links, as well as the advantages and limitations of both approaches.

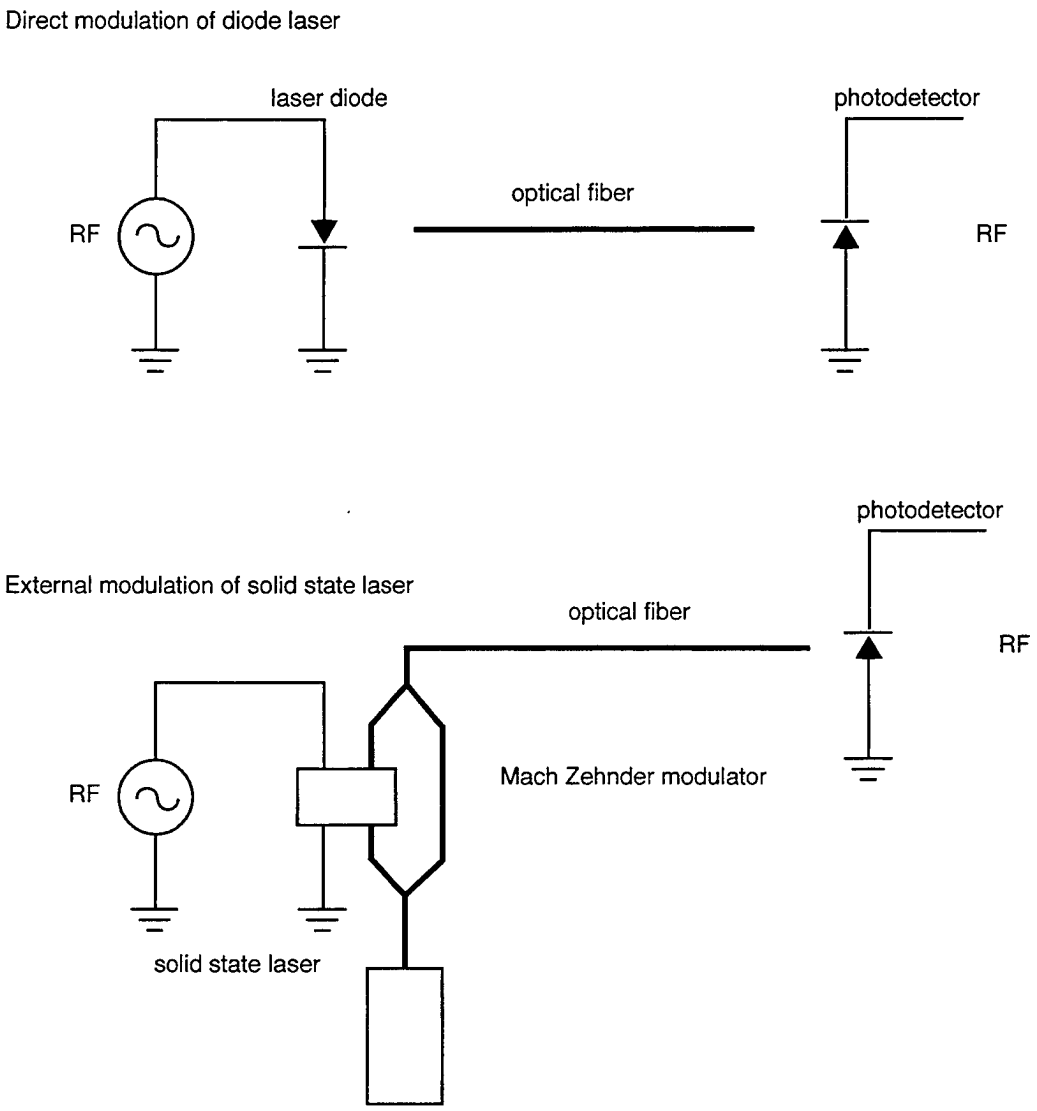

Figure 4.1 Optical Microwave Link

The signal to noise ratio in an analog photonic link is ultimately limited by the fact that the signal is carried by optical rather than by microwave photons. This fact has important consequences. For a conventional microwave link, thermal noise provides the ultimate limit to the signal to noise power ratio (SNR):

$$SNR_{\mu} = \frac{P_{\mu}}{k_B T \Delta f} \tag{4-1}$$

where P_{μ} is the microwave power, k_B is Boltzmann's constant, T is the absolute system temperature, and Δf is the bandwidth. Photon shot noise is suppressed in microwave signals because the occupation of photon quantum states is typically much greater than one, and detection is achieved coherently, i.e. the microwave signal acts as a classical wave. By contrast photon shot noise is typically the dominant noise mechanism in optical links, leading to a signal-to-noise ratio:

$$SNR_{opt} = \frac{P_{opt}}{2h\nu \Delta f} \tag{4-2}$$

where P_{opt} is the modulated optical power and $h\nu$ is the photon energy. Photon shot noise is present despite the fact that laser sources are coherent, because each photon is detected by the incoherent production of an electron-hole pair in the photodetector. (In principle photon shot noise can be avoided by using optically coherent detection, e.g. optical heterodyne detection, but this creates other difficulties and is seldom used in practice.) Comparing Equations (4-1) and (4-2) we find that a photonic link requires a greater power than a microwave link to maintain the same signal-to-noise ratio by the factor:

$$\frac{P_{opt}}{P_{\mu}} = \frac{2h\nu}{k_B T} \tag{4-3}$$

essentially the ratio of the photon energy to the thermal energy. An analysis of the quantity of information which can be carried by the two links leads to a similar result. For a typical photonic microwave link with wavelength $\lambda = 1.5\mu$m at $T = 300$ K, the power required for an ideal optical link is larger by the factor $P_{opt}/P_{\mu} \approx 60$ corresponding to a loss in signal-to-noise

ratio of 18 dB. For directly modulated links, this loss of SNR directly impacts performance, contributing 18 dB to the link noise figure. The performance of directly modulated links is currently limited by laser diode noise to much higher noise figures (~60 dB), as discussed below. For externally modulated links, loss of signal-to-noise can be compensated to some extent by higher laser power.

Because optical transmission requires greater power than microwaves to maintain the same signal-to-noise ratio, power handling of photonic devices and optical fibers becomes an important issue. The optical power handling capability of directly modulated lasers and microwave photodetectors is typically $P_{opt} < 10$ mW at present. This optical power corresponds to a compression-limited dynamic range $SNR_{opt} \sim (6 \times 10^4)^2$ or 96 dB for a typical 10 MHz bandwidth, comparable to the SNR achievable in current radars, but much smaller than the SNR achievable in conventional microwave links. Because the maximum power is near the limit required to maintain an acceptable signal-to-noise ratio, current detectors do not have a great deal of headroom to provide excess power handling to split (fan out) or combine (fan in) optical signals.

As an example, we consider a photonic link using a distributed feedback diode laser with power 10 mW and relative intensity noise RIN $= -150$ dB for 1 Hz bandwidth, corresponding to a compression limited dynamic range of 80 dB for a typical radar bandwidth $\Delta f = 10$ MHz. This dynamic range is good, but low enough that one would not want further degradation. For 10 mW laser power the photon shot noise floor is at -166 dB for 1 Hz bandwidth, giving a headroom of 16 dB in signal. Because the signal is represented by optical power rather than optical field, the headroom in optical power is only 8 dB corresponding to a fan out of 6 before the signal-to-noise ratio is degraded by photon shot noise. In order to increase the fan out without

degrading SNR, higher laser power or optical amplification is necessary, e.g. using Er-doped fiber optic amplifiers.

The ultimate limit to signal-to-noise ratio, fan out, and fan in is presented by the optical fiber itself. Stimulated Brillouin scattering limits the power which can be transmitted through a single mode fiber without attenuation. For moderate lengths $\sim$ 150 m of fiber the power is limited to $P_{opt} < 0.5$ W for a single laser line in a single mode fiber. The ultimate dynamic range of the optical fiber at this power due to photon shot noise from Equation (4-2) is $SNR_{opt} = (4.5 \times 10^5)^2$ or 113 dB with noise bandwidth $\Delta f = 10$ MHz. This dynamic range is better than the SNR of most current radars and is certainly very useful, but does not provide a great deal of headroom. As a result, passive fiber optic signal splitters and combiners have limited fan out and fan in. For the example above with signal SNR of 80 dB and 10 MHz bandwidth, the fan in or fan out of the fiber alone for passive splitters and combiners is limited to $\sim$ 300 before the signal-to-noise ratio is degraded.

The detection of small targets, such as fast low flying missiles in clutter, requires very high dynamic range; a dynamic range of 120 dB at 10 MHz is often used as a target. This specification approaches or exceeds the fundamental capability of a single analog photonic link set by the onset of nonlinearity and by photon shot noise. With existing components the situation is far worse, because current noise performance does not yet approach the shot noise limit. These limitations mean that the use of photonics for very high dynamic range radar should be examined very carefully.

Although the fan-in and fan-out of analog photonic components are generally large enough to be useful, they are far less than the number of elements in a phased array radar. The use of several stages of components with optical gain is necessary in order to maintain the signal-to-noise ratio of an analog signal in a large photonic system. The need for optical amplifiers compli-

cates photonic system design, and increases the cost and complexity of the system. Optical amplifiers also introduce additional noise which must be included in the noise budget for the system. The considerable loss encountered in making the transition from electronics to photonics and back is a strong incentive to keep the signal entirely photonic or electronic as is it processed by the system. Digital telephone systems commonly use a photodetector-electronic amplifier-diode laser combination to provide gain in long optical fiber transmission lines. This arrangement is inefficient and seems impractical for a photonic phased array radar, which would require a large number of amplifiers. More recently purely optical amplifiers have been developed, based on laser diode pumped Er-doped optical fibers. These are simpler and more reliable than their electronic counterparts, and seem better suited to photonic radar.

4.3.4 Laser Diodes

Laser diodes used for directly modulated photonic links have advantages and limitations which determine the characteristics of the link to a large extent. The advantages of directly modulated laser diodes are simplicity, small size, the potential for integrated optoelectronics, and potentially low cost (although the current cost is quite high ~$5k). Disadvantages are limited frequency response, and relatively high noise levels. Two types of laser diodes are considered here: Fabry-Perot (FP) laser diodes with a cavity defined by two partially reflecting plane mirrors, typically the cleaved ends of the device; and distributed feedback (DFB) lasers with a spatially extended corrugated reflector. Fabry-Perot diode lasers typically excite a number of cavity modes, while distributed feedback lasers excite only one mode and have narrower linewidth as a consequence of using a frequency selective mirror.

The frequency response of a laser diode is set by the relaxation oscillation frequency f_r, determined by the dynamics of photons and charge carriers within the laser cavity (see for example, Zmuda and Toughlian, 1994 [8]):

$$f_r = \frac{1}{2\pi}\sqrt{\frac{1}{\tau_p \tau_{stim}}} \tag{4-4}$$

where τ_p is the photon lifetime and τ_{stim} is the stimulated carrier lifetime. The frequency response of diode lasers can be optimized using Equation (4-4) as a guide. Quantum well lasers have demonstrated values of relaxation frequency into the mm-wave regime.

The dominant noise mechanism in laser diodes is relative intensity noise (RIN), which depends strongly on frequency, and can be calculated by adding random noise terms to the laser equations. Theoretical plots of the power spectrum of relative intensity noise for a single cavity mode are shown in Figure 4-2, with logarithmic axes. The RIN is peaked near the relaxation frequency of the laser, and falls to substantially lower values at lower frequencies if only one mode is excited. When a number of cavity modes are excited in a multi-mode laser the total power is stabilized, but power in a single mode can fluctuate leading to low frequency noise, shown as the solid lines in Figure 4-2 for two sets of parameter values. Any property of the optical system connected to a multimode laser which favors one cavity mode over another will uncover mode fluctuation noise. In order to achieve optimum noise performance, the optical cavity of laser diodes must be isolated from unwanted reflections from the optical system, typically by using an optical isolator.

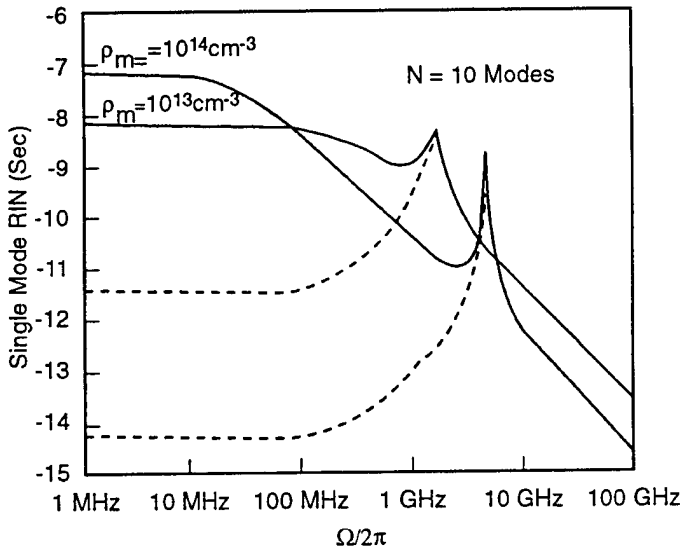

Figure 4-2. Theoretical estimates of relative intensity noise (RIN) for a single cavity mode, laser diode. At frequencies below the laser relation frequency peak the dashed lines are single mode and the solid lines are for multimode multimode laser diodes.

Fabry-Perot diode lasers, which typically operate multimode, have higher relative intensity noise [typically RIN $\sim$ (-135 to -140) dB/Hz] than single-mode distributed feedback laser diodes [noise typically RIN $\sim$ (-150 to -155) dB/Hz] (Cox 1995 [9]). Lower noise favors DFB laser diodes for directly modulated photonic microwave links, although their cost is currently somewhat higher than FP laser diodes. The RIN for both types peaks near the relaxation oscillation frequency making lower frequency operation desirable, and limiting the modulation bandwidth. These considerations argue against using directly modulated laser diodes at frequencies much above $\sim$ 10 GHz.

4.3.5 External Modulators

Externally modulated photonic microwave links combine a cw solid state laser with an external modulator. The solid state laser sets the noise floor

and contributes substantially to the size and weight of the system, while the modulator determines the frequency response and link gain. As discussed above, nonlinearity in the single mode optical fiber itself limits the maximum optical power to < 0.5 W per line of the laser. Multimode solid state lasers lasing on a number of lines can use correspondingly higher power.

Relatively compact, diode pumped YAG lasers are available with adequate power and low noise at microwave frequencies (RIN ~ -175 to -180 dB/Hz). Higher optical power, available for externally modulated links, can compensate to some extent for losses in signal-to-noise ratio associated with device efficiency and with the use of photonics as discussed above. However, the size, weight, and power consumption of solid state lasers limits their use in systems. Very small and efficient solid state lasers are currently under development, and could substantially broaden the range of applications for external modulated links.

Two general types of modulators are currently in use for microwave applications: Mach-Zehnder (MZ) interferometers and electro-absorption (EA) devices. A Mach-Zehnder interferometer consists of a fiber splitter, an optical phase shifter, and a combiner, as illustrated schematically in Figure 4-1. It operates by introducing an electronically determined phase shift between the two branches via the change in index of refraction induced by an applied voltage V. When the relative phase shift reaches π radians at a characteristic applied voltage V_π, the signals on the two branches cancel. The transfer characteristic of the modulator is inherently nonlinear, and distortion is minimized by a proper choice of bias voltage.

The performance of MZ modulators is determined by the electro-optic material and by the geometry of the device. The parameter V_π determines the microwave power necessary to modulate the optical carrier; in order to improve the link gain and noise figure, smaller values of V_π are desirable.

The parameter V_π in turn is proportional to the product of the electro-optic coefficient of the material and the optical path length of the interferometer. The intrinsic frequency response of materials currently in use is sufficiently high not to limit performance. In practice, the frequency response is determined by dephasing of the microwave and optical signals along the optical path inside the interferometer, due to their different velocities of propagation. Velocity matching of the optical and microwave signals inside the MZ modulator promises to increase both V_π and frequency response. Mach-Zehnder modulators with frequency response extending into the mm-wave region have already been demonstrated.

Lithium niobate ($LiNbO_3$) is the most common electro-optic material currently used in Mach Zehnder modulators; it is a rugged material and its properties are well understood, but it offers limited electro-optic responsivity. Current research directed at obtaining higher sensitivity (lower V_π) using new electro-optic polymers shows promise. However polymer materials are typically much less rugged than lithium niobate.

Electro-absorption modulators are based on the reduction of light intensity through absorption rather than destructive interference. The microwave electric field modulates the light intensity by changing the optical wavelength of a feature in the absorption spectrum of the device. A promising modulator for microwave applications is the multiple quantum well (MQW) self electro-optic device (SEED). Custom designed quantum well structures can be grown with atomic precision using ternary or quaternary III-V materials via modern techniques. As a consequence of reduced dimensionality, the exciton absorption in two-dimensional quantum wells yields a strong sharp optical absorption line even at room temperature. The wavelength of this line can be shifted substantially by the application of an electric field which spatially separates the electron and hole comprising the exciton. Because the width of the quantum well is very small, relatively modest applied volt-

ages produce large electric fields and wavelength shifts. The combination of strong absorption and strong wavelength shift permits fabrication of electro-absorption modulators of small size with attractive values of V_π, and reduces the importance of velocity matching of the microwave and optical fields. The shift in band-edge absorption with electric field via the Franz-Keldysh effect has also been used to make electro-absorption modulators.

Recent demonstrations of microwave modulators show microwave bandwidths reaching into the mm-wave region, with one demonstration of a bandpass modulator by Bridges operating at 94 GHz. The extinction voltage V_π is generally larger than one would like for MZ interferometers, and achieves the best values for multiple quantum well devices. The estimated microwave link gain of recent demonstrations is at best G ~ -10 dB and falls as low as G ~ -40 dB, i.e. there is considerable loss.

4.3.6 Photodetectors

The majority of photonic microwave links are based on incoherent detection of the optical signal by the absorption of photons and production of charge carriers in the photodetector. Compact semiconductor photodetectors with good quantum efficiency have been developed and perfected for a great variety of applications. The important issues for analog microwave links are high speed coupled with high power handing capability.

As discussed above, the dominant noise source in incoherent photodetectors is generally photon shot noise. In order to obtain the signal-to-noise ratio for photodetectors due to photon shot noise from Equation(4-2) we multiply by the overall efficiency $\eta = \eta_q \eta_m$ which is the product of the quantum efficiency η_q for converting a photon to charge carriers and the efficiency η_m

for extracting the carriers from the device at the microwave frequency.

$$SNR_{opt} = \frac{\eta P_{opt}}{2h\nu\Delta f} \,. \tag{4-5}$$

Here P_{opt} is the incident optical power, $h\nu$ is the photon energy, and Δf is the signal bandwidth. The quantum efficiency η_q of photodetector materials commonly approaches one. However, the efficiency η_μ can be much less due to cancellation of the microwave signal inside the device if the dimensions of active area approach or exceed the microwave wavelength. The requirements of high power and high efficiency for good signal-to-noise ratio thus conflict and require devices in which velocity matching of the optical and microwave signals is obtained.

Recent high speed photodetector demonstrations achieve bandwidths extending well into the mm-wave region. High speed alone is not sufficient for photonic microwave links, as discussed above, and the primary challenge is to obtain higher power handling capability without sacrificing too much speed. Relatively large devices are required for higher power handling, but these commonly have poorer overall efficiency due to cancellation of the microwave signal. Velocity matching of the optical and microwave fields in specially designed waveguide configurations is required to improve power handling while maintaining good bandwidth.

4.3.7 Photonic Time Delay Generation

A photonic microwave link that generates an adjustable time delay is proposed as a key part of true time delay radars. Many schemes for delay generation have been proposed. We outline a number of mechanisms here. Important criteria for delay generation mechanisms are simplicity and low component count. Seemingly straightforward schemes for time delay genera-

tion can lead to an explosion in the number of devices, complexity, and cost for a practical radar with many antenna elements, as discussed below.

Perhaps the most straightforward way to generate adjustable delays is to use a network of optical switches to add loops of fiber of varying lengths to the delay line. Advantages of this approach are that optical fiber is compact, light weight, and immune to electromagnetic interference — as for all fiber optic systems. Disadvantages are the need for many optical switches and the early state of optical switch design. Conversion to electrical signals and the use of electrical switches is argued against by the large conversion loss in current electro-optical devices.

Another class of photonic delay lines is based on the use of fibers with an adjustable index of refraction tuned by the optical frequency. The primary advantages of this approach is its relative simplicity — only one fiber is used for each channel, with no optical switches. Disadvantages are the need for a tunable laser and the long fiber length needed to generate a sufficiently large range of delays. The problem is to obtain a rapid change of index of refraction over a relatively small range of optical frequency. The Kramers-Kronig relation between the real and imaginary parts of the dielectric constant of a material means that strong dispersion can be obtained only at the expense of added absorption at the same optical frequencies.

An approach to delay generation we found particularly promising is illustrated in Figure 4-3. This scheme uses a single optical fiber with Bragg gratings with different periods located at various places along its length. Each Bragg grating reflects only one optical frequency, so that the delay can be adjusted between a number of discrete values by changing the optical frequency. The set of optical frequencies required can be quite closely spaced. Prof. Ming Wu of UCLA described a mode locked semiconductor laser which generates a comb of spectral lines suitable for this purpose. This system has

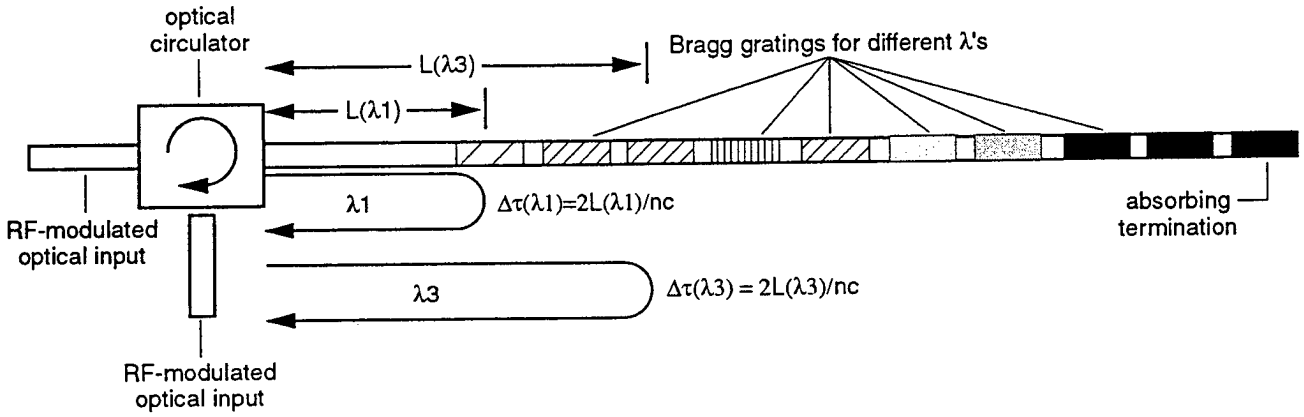

Figure 4.3 L. J. Lembo, et al., "Low-loss fiber-optic time-delay element for phased - array antennas," SPIE Vol. 2155 - Optoelectronic Signal Processing for Phased-Array Antennas IV, p. 13, 1994.

the advantages of the fibers with tunable index of refraction — simplicity and compactness — but provides a mechanism to generate widely differing delays. A remaining disadvantage is the need for switchable optical frequency.

4.3.8 Coherent Photonic Systems

We heard several talks at the summer study on optically coherent approaches to photonic radar. We considered this class of systems briefly and we only make a few general observations here. Coherent photonic systems have many advantages and offer greater flexibility in design than incoherent systems. In a coherent photonic system the signal is generally represented by the optical field, as in microwave systems, rather than the optical power. Building blocks of conventional microwave systems have analogs in coherent optical systems: heterodyne and homodyne mixers for frequency conversion and square law detectors, for example. Coherent optical signals permit sophisticated approaches to signal modulation and transmission such as suppressed optical carrier modulation schemes that are analogs of single- or double-sideband modulation of radio signals. Coherent systems can also escape the limitation on signal-to-noise imposed by photon shot noise. For these reasons coherent photonic radar has attracted much attention and is the subject of considerable research.

Coherent photonic systems also have serious drawbacks. Very tight constraints on mechanical performance apply if the coherence of the optical signal must be maintained across any sizable part of the system. Motion due to vibration, thermal expansion, etc. must be limited to a fraction of a wavelength across the system. These constraints also apply to thermal expansion of optical fibers. In the laboratory it is possible to maintain coherence using vibration isolated optical tables and thermal control. But for military

systems in the field the sensitivity of coherent photonic systems to vibration and thermal swings is a potentially serious problem. These limitations do not necessarily apply to all applications of coherent photonics, for example Mach Zehnder external modulators are self contained and transmission of signals via suppressed carrier modulation could be done without global phase coherence. Nonetheless, the maintenance of optical phase coherence is an important issue for any coherent photonic system which must be addressed in system design.

4.3.9 An Application for a Single Photonic Microwave Link — Antenna Remoting

Photonics can have important applications which are much more modest in scope than photonic phased array radar. Photonic devices have been used for antenna testing, for example by Toyon Research, because the optical fibers minimally perturb the electromagnetic field. A proposal presented by Charles Cox of Lincoln Laboratory is to use a photonic link to remotely locate an antenna in the field. The best site for an antenna is generally well away from the receive or transmit electronics and the operators; interaction between the many antennas aboard a ship or near a communication center is also serious issue. Because antennas are exposed to the elements and hostile fire, they should also be expendable and low-cost. Remote antennas using current photonic technology are projected to give good performance at moderate frequencies $\sim$ 100 MHz and could be fielded in the near future. Because they use only one photonic link, their cost can be relatively low.

In the example presented to us, a simple dipole antenna operating at 100 MHz is directly connected to an external modulator without a preamp. Both the solid state laser source and photodiode receiver are located with the receive electronics and operator; a loop of optical fiber connects them

to the remotely located antenna and modulator. At 100 MHz the minimum detectable field strength without a preamplifier is $\cong$ 2.3 μV/m, lower than the intrinsic sky noise of the antenna alone $\cong$ 4 μV/m, so that the photonic link causes little degradation of the signal. This system seems attractive because of its simplicity and potential low cost, and because the antenna can be located at considerable distances from the receiver. At higher frequencies the performance is less good, because the modulator sensitivity is poorer while the sky noise decreases. Operation at frequencies up to $\sim$ 400 MHz may be possible in the future.

4.4 The GEISHA Concept

Power amplifiers are a critical part of new phased array radar concepts, and improvements in amplifier technology can have a sizable impact on the cost and performance of the system. Many approaches to phased array radar require a transmit module at each antenna element. In arrays with hundreds or thousands of elements, a high premium is placed on the cost of these amplifiers. In addition, ultrawideband radar will also require amplifiers with comparably broad bandwidth and ultrahigh linearity in order to avoid intermodulation products.

At the summer study we were briefed on a promising new amplifier concept — GEISHA — which is an acronym for Gun, Electron Injection, for Semiconductor Hybrid Amplification. The projected specifications for this amplifier are ideally suited to use in ultrawideband radar arrays: the GEISHA device is planned to be physically compact, with high power ($\sim$ 40 W cw), ultrahigh linearity (intermodulation products > 28 dB below fundamental), high efficiency ($\sim$ 60% power added efficiency), and ultra-wide bandwidth ($\sim$ 100 MHz to 10 GHz). Figure 4-4 illustrates the concept — the

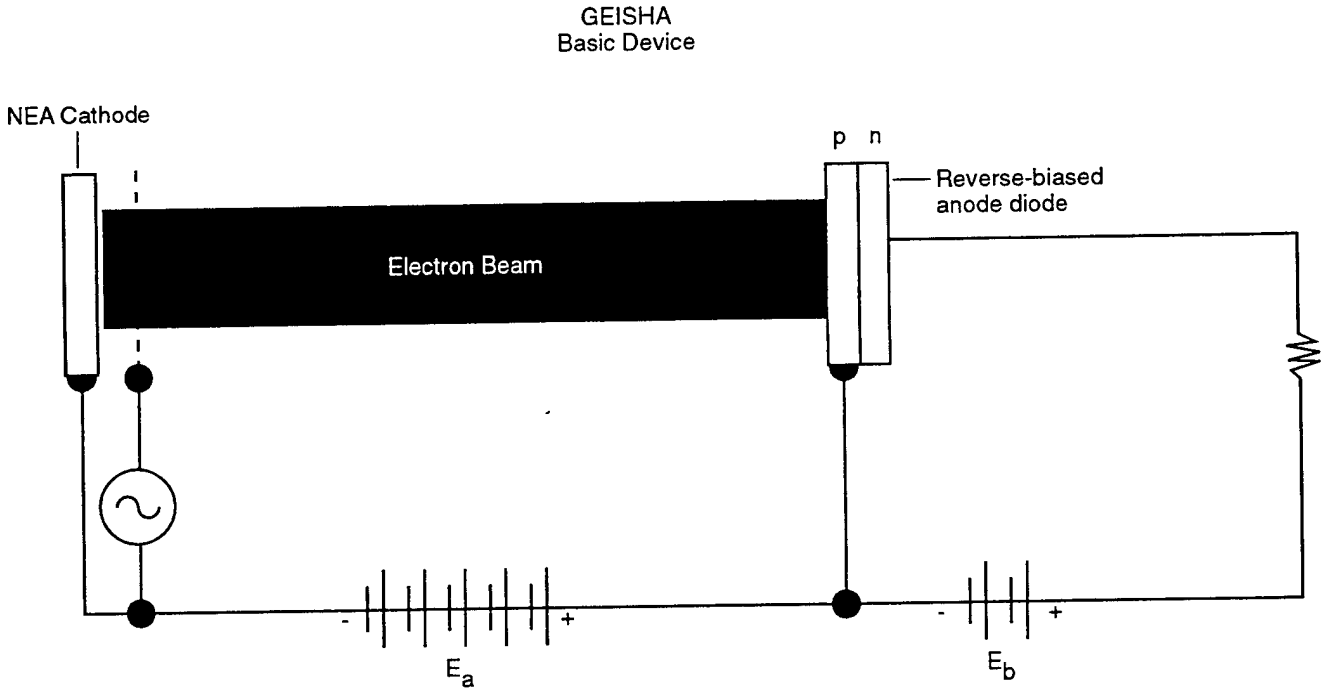

Figure 4.4 Schematic diagram illustrating the principal of a GEISHA (Gun, Electron Injection, for Semiconductor Hybrid Amplification) device.

GEISHA device is a vacuum tube with a specially constructed semiconductor cathode and anode which take advantage of recent progress in the area of wide bandgap semiconductors. The cathode is made from a negative electron affinity material and incorporates a base or gate to modulate the emitted electron beam current. The anode is a p-n junction which collects the electron beam and performs additional amplification via generation of many electron-hole pairs for each incident electron. The Miller capacitance in the equivalent circuit is minimized by grounding the p layer of the anode for improved high frequency response. The GEISHA concept is planned as a travelling wave device in order to obtain higher power. The signal is injected at one end of the long cathode, and the input signal, the modulated electron beam, and the anode current are all coherently modulated along the length of the device as a traveling wave, given appropriate velocity matching of the electromagnetic waves in all three regions.

The GEISHA concept is made possible by recent progress in the area of wide bandgap semiconductors. Wide bandgap materials (e.g. SiC, diamond, GaN, AlN) have many novel properties, including high dielectric strength and high thermal conductivity. For GEISHA their most important property is negative electron affinity (NEA) — due to the high bandgap, an electron placed in the conduction band has greater energy than in the vacuum outside. Negative electron affinity materials can make excellent cold cathodes, if one is able to form efficient contacts which inject electrons into the conduction band. We were told of recent experiments at Lincoln Laboratory in which electrons in the conduction band of diamond were internally accelerated to kV energies before leaving the material. While internal acceleration of electrons is not essential to the GEISHA concept, it could be a very useful approach which leads to even smaller devices.

We were impressed by the potent importance of the GEISHA concept for phased array radar and have the following recommendations:

- Pursue GEISHA research to fabricate working devices whose performance can be compared with other amplifiers.
- Support continued research in wide bandgap semiconductor materials — growth, characterization and processing.
- Develop efficient injecting contacts for electrons in wide bandgap materials, and investigate internal electron acceleration and high energy electron transport.
- Investigate the effects of electron beam damage and aging in semiconductor cathode and anode materials.

4.5 Ultra Wideband Antenna Considerations and Numerical Electromagnetics

4.5.1 Ultra Wideband Array Elements

Ultra wideband array antennas require special designs for the radiating elements. Such elements must not only have a low standing wave ratio over a very wide band, but also must meet various mechanical requirements, such as the low height profile required for a conformal array. Current conformal antennas are usually made using microstrip elements (dipoles or patches) (Munson, 1974) [2] and much progress has been made over the last two decades in this area (Zurcher and Gardiol, 1995) [4]. Dipole elements are inherently narrowband so patch elements of various shapes are used when wide bandwidths are desired. In the 1990's designs have emerged yielding bandwidths of a few tens of percent using multiple patches, that are either on a single level or stacked vertically. Strip-slot-foam-inverted patch (SSFIP)

technology with stacked, but still very thin, patches has allowed bandwidths as wide as 33% at X-band, i.e. from 8 to 11.3 GHz with a standing wave ratio (SWR) of less than 2 (Zurcher and Gardiol, 1995) [4].

The Lockheed-Martin approach briefed to JASON consisted of a structurally-embedded, photonically-controlled phased array antenna (SEPCPAA) in which photoconductive patch elements were stacked several layers deep to cover the range 1 – 18 GHz. Figure 4-5 illustrates the concept. It is not clear from the information available just how the approach is to be implemented. However, some general comments can be made. First, a log periodic array of elements in photoconductive silicon is to be used with a stack four layers deep shown. In the literature stacks of patches have certainly been used to obtain broad bandwidths, but the SEPCPAA concept, as we interpret the diagrams, calls for much greater percent bandwidths, i.e. > 60 to 80%, – this is a challenging goal. The concept proposed uses multiple layers of stacked patches. In such a situation the role of surface and leaky wave propagation along and between layers needs to be carefully considered since undesired coupling between elements can seriously erode element and array performance. The numerical EM techniques discussed in Section 4.5.2 below should be helpful in both evaluating and, if warranted, fabricating the concept of Figure 4-5.

In array design the selection of substrate material is crucial if large array areas are needed and low cost is desired. Military antennas need to stand up to severe environments and substrate materials that are low cost and low loss may not be suitable, e.g. polypropylene is both low cost and low loss, but has a low melting point.

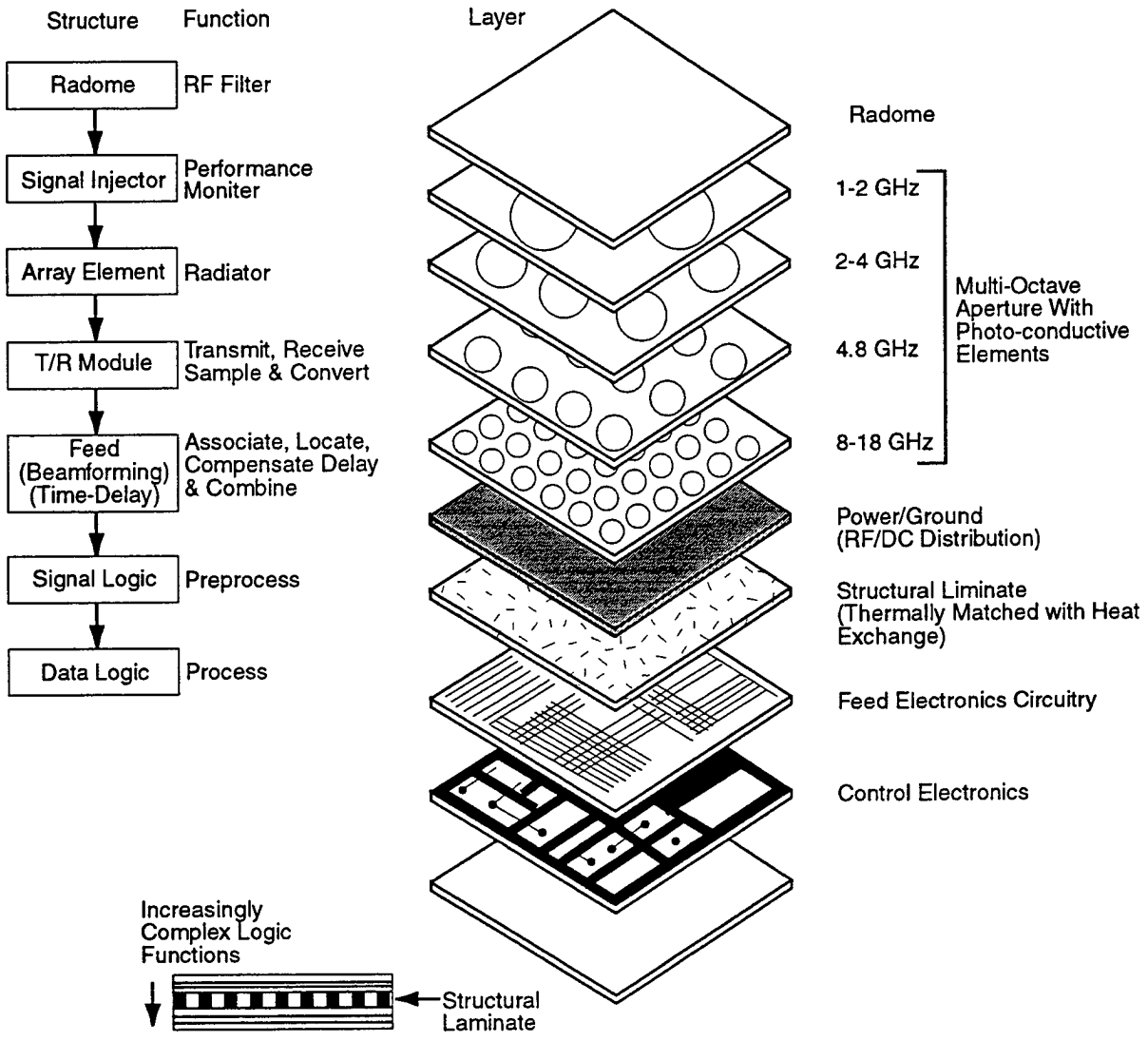

Figure 4-5. Lockheed Martin approach to a structurally embedded photonically controlled phased array antenna (SEPCPAA). This approach features a multiple layer scheme with photoconductive silicon elements that cover an octave waveband in each layer.

4.5.2 Application of Numerical Electromagnetics to Wideband Array Antennas

The design of sophisticated multilayer patch antennas is an intricate process, requiring a number of material and configuration trade-offs. Complex electromagnetics problems can be attacked by experimental, analytical and numerical techniques. Experimental methods are the most conclusive, but are usually expensive and cover only a small range of parameter space. Analytical techniques are available for only a small number of problems. Numerical techniques are a relatively recent tool, but the current state of the art is sufficiently advanced that a wide variety of applications are possible (Sadiku, 1992) [5]. We recommend the use of numerical electromagnetic techniques, e.g. finite element, method of moments and the like, as tools in the design process of wideband array antennas. For example, we think that numerical EM would be useful in research on complex wideband designs, such as shown in Figure 4-5. Numerical simulations could be helpful in deciding what types (configurations and materials) of array elements to fabricate for experimental testing – numerical EM would also be helpful in understanding experimental results. Thus, both theoretical modeling and laboratory experiments play important roles in arriving at an effective wideband array design. Further, numerical EM calculations would be useful in studying the interaction of array elements and the isolation of transmit and receive apertures.

Numerical electromagnetic techniques allow one to perform experiments by simulation rather than by physical construction of an antenna. Thus, the SWR of an antenna can be computed by modeling a structure, applying an excitation voltage at a partiuclar frequency and calculating the forward and reflected power between the exciter and the antenna. A variety of numerical EM methods are available as follows:

1. Finite element method (FEM)
2. Method of moments (MOM)
3. Finite difference method
4. Spectral methods
5. Method of weighted residuals
6. Transmission-line modeling
7. Monte Carlo method.

One point we want to stress here is that numerical methods can be highly accurate if properly applied – and there is considerable art in the application process. In Figure 4-6 we compare results of numerical EM calculations (Volakis, 1995) [6] with experimental measurements by NASA Langley Research Center. The figure shows normalized radiated power from a wrap-around, cavity-backed rectangular patch antenna on a cylinder ogive. The radiated power is calculated in two ways – a boundary integral and an absorbing boundary condition (ABC). The numerical EM scheme used is a hybrid FEM scheme (Gong et al., 1994). Note the close correspondence between the experimental measurements and the numerical EM results. We also point out that the antenna element is rather a complex device in a difficult conformal geometry.

Our point here is that numerical EM can be a significant money saver in the development of complex wideband antenna arrays. The idea is to use numerical EM to stimulate and later assess ideas for wideband arrays, such as shown in Figure 4-5. A numerical EM analysis of a proposed structure can reveal faults and strengthen a design before it is fabricated, thus saving the cost of fabricating designs with poor performance. Once a design is

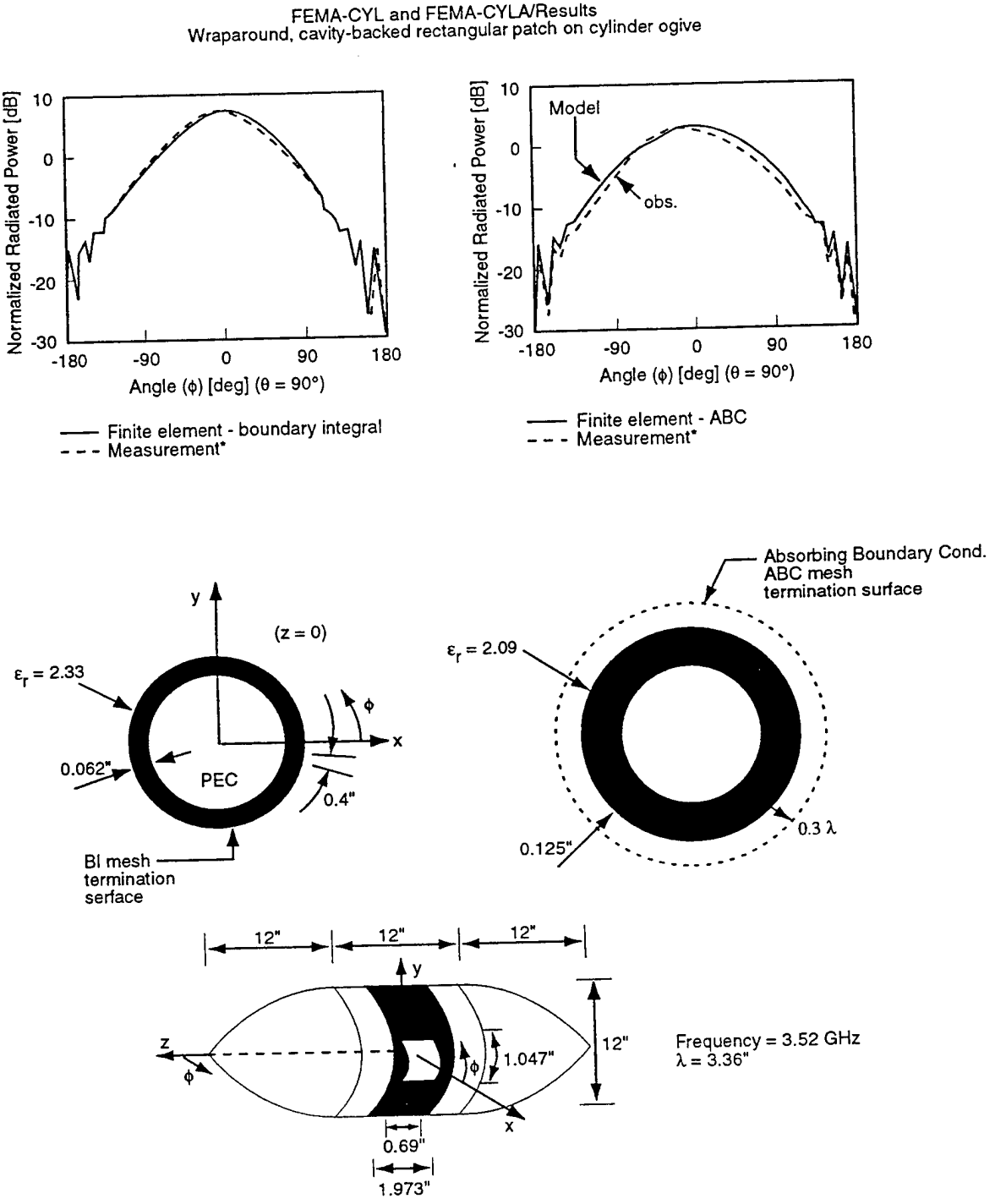

Figure 4-6. Comparison of numerical EM results and laboratory measurements for a wraparound, cavity-backed rectangular patch on a cylinder ogive (Volakis, 1995) [6].

fabricated and tested, numerical EM can help one understand anomalies in the test results and correct them.

4.5.3 Jamming and other Considerations

Wideband antennas are more vulnerable to jamming than narrowband antennas in that a jammer might be able to jam one antenna function by getting into the RF system via another function. With a wideband antenna a jammer can operate in both direction and frequency space. For example, a radar pointing in direction A might be jammed by putting power into the radar receiver RF system via an antenna beam being used for communication at another frequency that happens to point at the jammer. The jammer power could be at the communications frequency, not the radar frequency, and still disrupt radar performance by saturating a wideband receiver front end or by creating intermodulation products that fall in the radar bandpass.

5 WHAT'S MISSING AND NEXT GENERATION ISSUES

The two items that we think are missing in the program, as constituted in the summer of 1995, are systems engineering and integration of new technology into prototype radars. Clearly the development of new technology for advanced microwave radars is useful. However, priorities for the several technologies can not be effectively assessed without a systems approach. One way of implementing a systems study would be to develop radar system designs for say 5, 10 and 15 years into the future. This would allow Navy planners to know the options they have in terms of inserting advanced technology to obtain better performance and how other parts of the system need to be altered to accommodate the new technology. The second item is integration of new technology into prototype radars. Clearly this is the acid test for a technology. We recommend one such integration above, i.e. integration of an ultra stable local oscillator into a Doppler radar so that the level of ocean clutter at Doppler shifts of many kHz can be observed.

In terms of the overall objective of protecting Navy assets from cruise missile attack we see three ideas for the next generation, namely:

1. Addition of IR sensor data into the detection, tracking and homing functions. While IR sensors cannot operate under all weather conditions, the addition of IR sensors puts significant extra stress on a hostile cruise missile system in terms of decoys, deception, etc.

2. Use of multistatic radars to defeat stealth technology and provide redundancy. Here we are thinking of illumination by aircraft, such as high flying UAV's, or even satellites and reception by receivers on multiple air and surface platforms.

3. Use of HF (decameter wavelength), ground wave radars, monostatic and especially bistatic. HF radar can propagate over the horizon out to tens and even hundreds of km via ground wave and because of its large wavelength increases the difficulty of stealth technology. It is also relatively inexpensive. Bistatic operation could improve the azimuth resolution that is currently limited by arrays the size of a ship.

6 SUMMARY AND CONCLUSIONS

We summarize our principal findings and recommendations as follows:

1. We strongly recommend that radar and broader (ship air defense) system studies be an important part of this research program. Such studies should include the following:

   (a) Assessment of the dynamic range (subclutter visibility) needed to counter projected threats as well as the best system architectures to achieve these dynamic range requirements (see examples above in Section 3 and 4). One needs to know both how much 'subclutter visibility is needed' to counter a likely threat and where the environmental limits on the 'noise floor' are. Second, there are a variety of ways of obtaining the needed subclutter visibility. The system and particularly the signal processing architecture strongly impact analog to digital converter device requirements.

   (b) Assessment of how wide a bandwidth can actually be used due to factors outside radar technology, e.g. radio frequency interference, and the value of the extra bandwidth in terms of the radar's mission.

   (c) Study of the leverage of specific technologies with respect to radar performance – to help research priorities.

   (d) Preliminary design of advanced radar systems incorporating ACI technologies expected to be available in 5, 10 and 15 years to allow Navy planners access to the likely results of this project.

   Further we suggest that in assessing the potential of airborne radar, one should not neglect studies as to how much benefit could be obtained from better use of the warning time provided

by mast-top radars. After all there are going to be situations when airborne radars are not available and one is forced to rely on mast-top radars.

2. Advanced technologies, such as photonics, high temperature superconductor electronics, wide bandgap semiconductor devices and integrated antennas have great potential to improve radar performance and ultimately reduce cost.

3. 'True time delay' (TTD) beam forming, as currently implemented with less than N^2 independent time delays, is broadband and avoids squinting; but, used alone, doesn't allow for effective adaptive beam forming or multiple beams (in a single array).

4. Opto-electronic delay techniques may be best suited to simple phased array radars, while hybrids with direct digital synthesis are likely to be required for high performance radar requiring adaptive beam forming. We recommend consideration of a system involving direct digital synthesis of the outgoing radar signal at each array element – allowing very flexible digital control of a phased array radar. This HICAPOR concept is described in some detail above (Section 3).

5. High temperature superconductor stable local oscillators (STALOs) are now working in the laboratory – we recommend building a simple Doppler radar with one and observing targets and clutter to assess the impact of this device on the Doppler noise floor in a real clutter environment.

6. Gun, electron injection for semiconductor hybrid amplification (GEISHA) devices could be a very useful technology, especially for wideband transmit/receive modules if device lifetime is not too limited and ultra linearity requirements can be met.

7. Ultra wide bandwidth array antennas are a useful goal, but a systems study is needed to assess how wide a bandwidth can actually be used due to factors outside radar technology and the value of the extra bandwidth. In the photonically controlled, stacked patch concept briefed to JASON we point out that the bandwidths suggested ($\approx$ 60 to 80%) are a significant jump from existing techniques and that surface waves propagating along and amongst the layers in the array may degrade performance. We recommend the use of numerical electromagnetic modeling to assess the feasibility of the proposed concept and, if feasible, to help in finding effective materials and configurations to implement the concept.

A APPENDIX — ASSESSING BROADBAND PROCESSING

It seems that the day of broadband signal processing has arrived, especially in radar and sonar. In radar, the advent of photonic control has suggested true time delay steering, which is automatically squintless at all frequencies; in sonar, quieter submarines means squeezing as much information as possible out of the broadband transmitted signal.

Now a broadband array may be viewed as one which operates well at each of a large and widespread number of individual frequencies, or one that accurately measures and responds to a signal which is broadband in character. We are largely interested here in the second sort.

The return from a cruise missile illuminated by a pulse is of this character. Also of this nature is the generalized pump noise, hull noise, flow noise produced by a submarine.

Now it seems to us that many of the usual measures of processing efficiency no longer make sense for broadband processing, nor do the usual procedures of placing nulls or adaptively steering the array to eliminate clutter. Moreover, there does not appear to be a satisfactory theory to fill in these newly arisen voids in our knowledge.

In this paper we make a start towards such a theory. It will be of a fairly abstract and very general character; only one numerical example has been worked out, and this of an artificial character. Our treatment will include matched field processing and adaptive beamforming, but without any discussion, largely meaningless for broadband processing, of beam shape, main lobe and nulls. In fact we are not going to form beams at all; instead

all of our measures of performance are probabilistic in nature — principally log likelihood and variances.

In Section 3 of this report we described more conventional "beamforming" approaches when there are some tuneable parameters in the array, such as time delays or complex phase modulators.

In order to keep the discussion strictly probabilistic we make an assumption about signal source, which is as a matter of fact the novel feature in this treatment.

We assume that the signal source is a sample path from a weakly stationary stochastic process and that the signal statistics are purely Gaussian. For our purposes this means that the second order statistics (i.e. covariance) determine the process entirely. (The assumption of Gaussian statistics could with some difficulty be replaced by other assumptions, but the computational burden will increase accordingly.)

Provided appropriate assumptions are made the method will work for several signal sources, each with their own stochastic process description.

One might ask where the stochastic assumptions on signal source come from. In the examples we currently envision, the answer is ignorance. The simplest assumption reflecting ignorance is that of a flat power spectrum over a range of frequencies of interest — for sonar 200 to 700 hertz might be suitable. Choices in radar will depend on special situations. If the source is narrow band, we may simply take the power spectrum as a delta function. With experience gained from time and experimentation better choices of power spectrum might be available, tapered for example. The autocovariance of the signal source is, of course, the Fourier transform of power spectrum.

Our sensor array, locations known, will have no particular geometry, it

could be linear, planar, or random, but we do have to make an assumption about geometry at the start of the processing, time $t = 0$. In sonar, this assumption will be the localization of the source in a voxel in a 3D-lattice. In radar bearing analysis it will be, for one example, the pitch of the plane wave front and its location in space at time $t = 0$. In a systematic search, the initial assumption will vary as the procedure explores the geometric space available.

Given the geometric data just described, one may next, using matched field analysis if desired, give the excitation at each sensor as a function of time. Dissipation and multipath may be taken into account. What this construction means mathematically is simply that the excitation at each sensor is a *known linear filter* applied to the signal.

So much for the sensors and the signal source. Next we have to describe the background noise field. Here we make the usual assumption of a Gaussian field — each sensor is receiving a weakly stationary Gaussian noise. The noise may partly be the result of surface ships, or of other targets in the radar case. What we must know for the analysis is the cross variance of each sensor with every other at all temporal offsets, or equally well, the cross variance of each with every other in every frequency bin. The noise field statistics are to be computed and updated in the usual manner.

We have given ourselves enough information, and assumed enough, to compute exactly the following. Given a period of observation, what is the ratio of the probability density of signal present to no signal present. The logarithm of this ratio is our statistic for measuring presence of signal. We also are able to compute the *spread* (expected value of the statistic in signal present case minus expected value in signal absent case), and the *variance* in the signal absent case. Thus we can construct ROC curves for said statistic to be used in thresholding.

Now the reader may ask what all this is good for. Granted the assumptions we have made, the log likelihood is probably the strongest statistic available for detection. To the extent Neyman-Pearson theory holds here, for fixed detection probability, log likelihood yields the lowest false alarm rate. The performance of any other statistical procedure can be measured by comparing its strength with that of the log-likelihood.

One possible problem with the log-likelihood procedure is the volume of number crunching and signal processing it requires. It is probably manageable in sonar processing which is a relatively relaxed environment, except perhaps for the size of the search space.

In traditional sonar and radar processing, a linear predictor of signal present is the most familiar. We shall also describe in this report how to construct a maximum log-likelihood signal predictor, which is significantly more involved than the familiar techniques in the literature, but which is still readily compatible with an array architecture using time delay steering.

The analysis will be carried out independently in both the frequency and the temporal domains. The alert reader may ask what possible difference can this make — after all a max likelihood estimator is a max likelihood estimator. Actually there is a difference and it shows up in the way the observed data are handled. In a frequency analysis, the data is broken up into temporal chunks each long enough to extract the requisite frequency data, each chunk then yielding its own log-likelihood, which are then combined incoherently. In a temporal analysis, the whole observed data stream is analyzed coherently.

It is time to begin the analysis.

A.1 Log-Likelihood in the Frequency Domain

First, a temporal chunk, long enough to resolve frequencies of interest at Nyquist sampling rate, is frequency binned, say bins 1 to B. Say there are N sensors, and suppose

$$N(k) = (N_{i,j}(k)), \quad 1 \leq i,\ j \leq n\ ,$$

is the noise (sample) covariance matrix in the k^{th} frequency bin. A bearing or location of source having been assumed, the signal covariance matrix in the k^{th} bin, at the sensors, is a rank one Hermitian matrix $D(k)$, determined from the power spectrum at the k^{th} frequency plus multipath and attenuation. Suppose the observed data in the k^{th} frequency bin form a vector $\theta(k)$ whose components are the observed complex amplitudes at k^{th} frequency bin in sensor j, $j = 1, 2, \cdots, n$.

The probability density of the observation in the k^{th} bin, given signal present is:

$$\frac{1}{(2\pi)^n}\det(N(k)+D(k))e^{-\frac{1}{2}\theta(k)\{N(k)+D(k)\}^{-1}\theta^*(k)}$$

with a similar expression for probability signal absent.

Since the observations in distinct frequency bins are independent, the total log-likelihood is, up to an irrelevant constant:

$$\frac{1}{2}\sum_{k=1}^{B}\theta(k)[N^{-1}(k)-[N(k)+D(k)]^{-1}]\theta^*(k)+\sum_{k=1}^{B}[\ln\det(N(k)+D(k))-\ln\det N(k)]\ .$$

By a well known formula of Maybury, the above may be rewritten:

$$\frac{1}{2}\sum_{k=1}^{B}\frac{1}{1+TrN^{-1}(k)D(k)}\theta(k)N^{-1}(k)D(k)N^*(k)\theta^*(k)+\sum_{k=1}^{B}\ln(1+TrN^{-1}(k)D(k))\ ,$$

where Tr means matrix trace.

For the purpose of thresholding and getting ROC curves, the second summand above is irrelevant. But if we bear in mind that the whole expression is a log-likelihood, it could be mildly useful in a priority ordering of the various signal source locations. (We do not analyze this possibility.) For the purpose of thresholding and ROC construction, we simply take the statistic

$$X = \sum_{k=1}^{B} \frac{1}{1 + TrN^{-1}(k)D(k)} \theta(k)N^{-1}(k)D(k)N^{-1}(k)\theta^*(k) \ .$$

The expected value of X in the signal present and signal absent case are readily found, by noting for example, that the expected value of $\theta^*(k)\theta(k)$ in signal present case is $N(k) + D(k)$. Thus the *spread* is

$$\sum_{k=1}^{B} \frac{Tr^2(N^{-1}(k)D(k))}{1 + Tr(N^{-1}(k)D(k))} \ .$$

The variance of X in the signal absent case is readily computed by a familiar manipulation for finding higher mixed moments in multivariate normal distributions. Some care must be taken since variates are complex Gaussian, but the variance in question is found to be

$$\mathrm{Var}X = \sum_{k=1}^{B} \frac{Tr^2(N^{-1}(k)D(k))}{[1 + Tr(N^{-1}(k)D(k)]^2} \ .$$

The statistic X may be thrown into a form a little more computationally useful. Namely, since $D(k)$ is a rank one Hermitian matrix, we may always write it as $D(k) = d^*(k)d(k)$, with $d(k)$ a row vector, components unique up to constant phase change. Now

$$X = \sum_{k-1}^{B} \frac{|\theta(k)N^{-1}(k)d^*(k)|^2}{1 + d(k)N^{-1}(k)d^*(k)} \ .$$

The "natural" version of $d(k)$ is computed of course from matched field processing, involving just attenuation and multipath.

A.2 Linear Detection in the Frequency Domain

The statistic X of the last section requires a fair amount of computation; it is not of the form more commonly used in detection — that is linear detection. Here one takes a weighted sum of sensor excitations and its modulus squared is the detection number. We do not seek a good statistic of this sort in our analysis, but we can obtain a useful statistic of a quite similar nature. What we do is ask for a maximum likelihood estimate of the complex amplitude in the k^{th} frequency bin at the signal source.

Let us suppose that the true complex amplitude in the k^{th} frequency bin at signal source is $t(k)$. Then the amplitude in the k^{th} bin at the v^{th} sensor is $t(k)\alpha(v)$; $\alpha(v)$ is known from attenuation and multipath matched field processing. The log probability density of the time signal frequency content is the vector $t(k)$ that is, up to an irrelevant summand:

$$-\frac{1}{2}\left\{\sum_{k=1}^{B}\frac{|t(k)|^2}{\sigma^2(k)}+\sum_{k=1}^{B}[\theta(k)-t(k)\alpha]v^{-1}(k)[\theta(k)-t(k)\alpha]\right\}$$

where v is the vector $\alpha(1),\alpha(2),\cdots,\alpha(n)$, and $\sigma^2(k)$ is power spectral density in the k^{th} frequency bin.

The expression in curly brackets is to be minimized by one's choice of all $t(k)$'s; the minimum is uniquely attained and easily computed. We are not, just now, exactly interested in its exact computation, solely that its form is $t(k) = \theta(k)\cdot R^*(k)$, where $R(k)$ is for each k a row vector $R^1(k), R^2(k),\cdots,R^n(k)$. $\theta(k)$ is also: $\theta(k) = (\theta^1(k),\theta^2(k),\cdots,\theta^n(k))$. $\theta^1(k)\overline{R^1(k)}$ is the Fourier transform of a linear filter applied to first sensor, similarly for $\theta^2(k)\overline{R^2(k)}$, etc. Thus, the signal at the signal source has as its maximum likelihood estimate a linear filter (temporal) applied to the first sensor plus a linear filter applied to the second plus etc. This is a somewhat more familiar architecture for signal estimation, and possibly can be accommodated with

weighted sums of entries of tapped delay lines in each sensor, though some buffering may be necessary, since the filters may not be causal, and the delay lines may be very long.

We do not go into details here. The whole setting will be reviewed and revealed when we do likelihood analysis in the temporal domain.

A.3 Log-Likelihood and Linear Signal Detection in the Temporal Domain

We take the whole signal at source over the longest period of time for which the situation is stationary. If the source is moving in a known or assumed manner, this may be incorporated into processing. Suppose the signal, digitized for ease of analysis here, is $s(t)$, $t = 0, 1, 2, \cdots, K$. Signal covariance is assumed completely known. There is a matrix $Q(v)$ such that $sQ(v)$ is the induced signal at v^{th} sensor after matched field processing. Since $Q(v)$ just represents a linear filter, the columns of $Q(v)$ drift down, enclosed by zeros.

Let $\theta_1, \theta_2, \cdots, \theta_n$ be the observed data streams at the 1st, 2nd, $\cdots$, n^{th} sensor respectively. The noise covariance matrix N is made up of $K \times K$ blocks $N(i,j)$, $1 \leq i,\ j \leq n$, with $N_{ij} = \langle \theta_i^* \theta_j \rangle$, the expectation being taken with no signal present. The corresponding block for the signal data streams at sensors is $D_{ij} = Q^*(i)CQ(j)$, where C is the pure signal covariance. (Everything in sight here is real, but we still use * for conjugate transpose.)

The log-likelihood statistic to use here is then:

$$(\theta_1, \theta_2, \cdots \theta_n)\{N^{-1} - (D+N)^{-1}\} \begin{pmatrix} \theta_1^* \\ \theta_2^* \\ \vdots \\ \theta_n^* \end{pmatrix},$$

an expression which cannot be simplified as readily as in the previous treatment, because D is not rank one. The spread and variance, while readily computed, still involve the inverses of N and $D+N$. There is a well-known rapid method for computing N^{-1} on the fly as N is estimated by sampling, but this technique will not help with $(D+N)^{-1}$, unless the signal itself can be simulated on the fly as N is being estimated by sampling. Save perhaps in special cases, signal processing on the temporal side loses out to frequency side processing.

There is a slightly different way of writing the log-likelihood, which will be useful in a moment. Let P be N^{-1} with P blocked as was N. Except for a scale factor, the probability density that the raw signal was s and the observation was $\theta_1, \theta_2, \cdots, \theta_n$, is .

$$e^{-\frac{sC^{-1}s^*}{2}} e^{-E/2}$$

where E is given by

$$E = (\theta_1 - sQ(1), \theta_2 - sQ(2), \cdots, \theta_n - sQ(n))N^{-1}(\theta_1 - sQ(1), \cdots \theta_n - sQ(n))^*$$

Integrating out over s (simply complete the square), gives the probability density for the observation, given signal present, in a somewhat different form than previously. Integrating out over all s except for one component, gives the probability density for that component, from which its maximum likelihood estimate may be formed. It is somewhat easier to give the maximum likelihood estimate for the whole signal. Write E as

$$\sum_{v,u} [\theta_v - sQ(v)] P_{vu} [\theta_u - sQ(u)]^*$$

$$= \sum_{v,u} \theta_v P_{vu} \theta_u^* - 2s \sum_{v,u} Q(v) P_{vu} \theta_u^* \cdot + s \sum_{v,u} Q(v) P_{vu} Q^*(u)\ s^*$$
$$=: a - 2sb^* + sVs^*$$

The max likelihood estimate of s is then given by $s = b(C^{-1}+V)^{-1}$. This is to be contrasted with the much more numerically manageable estimate of s given in the frequency domain. In the temporal domain we have to invert the matrix N (which is $nK \times nK$), though this might be managed on the fly, and also invert $C^{-1} + V$, which is $K \times K$, and must be inverted honestly, as in the case with C. V being dependent on source location, the inversion of $C^{-1} + V$ is a multiple repeating task.

Next, the maximum likelihood estimate of any component of s involves no less computation, and no more, than that of all of s. This is simply a reflection of the fact that the max likelihood estimate of all of any collection of multivariate normal variables is the expected value of each.

The apparent advantage gained in temporal side processing of using the whole data stream is more than offset by the additional computation burden, particularly that of inverting large matrices.

There are a number of ways of circumventing these difficulties. One is to limit artificially the record size to say $K = 100$, and learn to live with frequent inversion of 100×100 matrices. The formula $s = b(C^{-1} + V)^{-1}$ produced earlier now estimates the 100 entries of s in terms of 100 entries of each sensor's received signal, the first entry of s estimated by later sensor signals, the last by earlier, the middle by half forward, half backward, thus being a form of Wiener "interpolatory" prediction. Architecturally, this is readily effected by 100 element long tapped delay lines in each sensor, with real (not complex) tapping constants.

Another approach might simply forget external noise, and construct once and for all the noise covariance matrix as due to array element cross talk and thermal noise.

While the temporal processing with tapped delay lines looks to be a possible attractive use of the now strongly promoted photonic delay lines, it seems that overall, frequency side processing is best, and not even for just signal estimation, but for detecting the presence of a signal using the statistics developed here earlier which depend quadratically on the sensor data.

References

[1] Flory, C. A. and R.C.Taber, Microwave oscillators incorporating cryogenic sapphire resonators, IEEE Proc. Int. Frequency Control Symp., 763-773 (1993).

[2] Munson, R. E., Conformal microstrip antennas for microwave phased arrays, IEEE Trans. Antennas Propagat. AP-22, 74-78 (1974).

[3] Shen, Z-Y, High-Temperature Superconducting Microwave Circuits, Artech House, Boston (1994).

[4] Zurcher, J. F. and F. E. Gardiol, Broadband Patch Antennas, Artech House, Boston (1995).

[5] Sadiku, M. N. O., Numerical Techniques in Electromagnetics, CRC Press, Boca Raton, Fl (1992).

[6] Volakis, J. L., private communication (1995).

[7] Microwave J. (1995).

[8] Henry Zmuda and Edward N. Toughlian Eds., Photonic Aspects of Modern Radar (Artech House, Boston, 1994).

[9] Cox, C.H., JASON Briefing, San Diego, Ca, Summer 1995.

DISTRIBUTION LIST

Director of Space and SDI Programs
SAF/AQSC
1060 Air Force Pentagon
Washington, DC 20330-1060

CMDR & Program Executive Officer
U S Army/CSSD-ZA
Strategic Defense Command
PO Box 15280
Arlington, VA 22215-0150

Superintendent
Code 1424
Attn Documents Librarian
Naval Postgraduate School
Monterey, CA93943

Director
Technology Directorate
Office of Naval Research
Room 407
800 N. Quincy Street
Arlington, VA 20305-1000

DTIC [2]
8725 John Jay Kingman Road
Suite 0944
Fort Belvoir,VA 22060-6218

Dr A. Michael Andrews
Director of Technology
SARD-TT
Room 3E480
Research Development Acquisition
Washington, DC 20301-0103

Dr Albert Brandenstein
Chief Scientist
Office of Nat'l Drug Control Policy
Executive Office of the President
Washington, DC 20500

Dr H Lee Buchanan, I I I
Director
DARPA/DSO
3701 North Fairfax Drive
Arlington, VA 22203-1714

Dr Collier
Chief Scientist
U S Army Strategic Defense Command
PO Box 15280
Arlington, VA 22215-0280

D A R P A Library
3701 North Fairfax Drive
Arlington, VA 22209-2308

Dr Victor Demarines, Jr.
President and Chief Exec Officer
The MITRE Corporation
A210
202 Burlington Road
Bedford,MA01730-1420

Mr Dan Flynn [5]
OSWR
Washington, DC 20505

Dr Paris Genalis
Deputy Director
OUSD(A&T)/S&TS/NW
The Pentagon, Room 3D1048
Washington, DC 20301

Dr Lawrence K. Gershwin
NIC/NIO/S&T
7E47, OHB
Washington, DC 20505

Dr. Helmut Hellwig
Deputy Asst Secretary
(Science, Technology and Engineering)
SAF/AQR
1919 S. Eads Street
Arlington, VA 22202-3053

DISTRIBUTION LIST

Dr Robert G Henderson
Director
JASON Program Office
The MITRE Corporation
1820 Dolley Madison Blvd
Mailstop W553
McLean, VA 22102

J A S O N Library [5]
The MITRE Corporation
Mail Stop W002
1820 Dolley Madison Blvd
McLean, VA 22102

Dr Anita Jones
Department of Defense
DOD, DDR&E
The Pentagon, Room 3E1014
Washington, DC 20301

Mr. O' Dean P. Judd
Los Alamos National Laboratory
Mailstop F650
Los Alamos, NM 87545

Dr Bobby R Junker
Office of Naval Research
Code 111
800 North Quincy Street
Arlington, VA 22217

Dr. Martha Krebs
Director
Energy Research
1000 Independence Ave, SW
Washington, DC 20858

Dr Ken Kress
Office of Research and Development
809 Ames Building
Washington, DC 20505

Lt Gen, Howard W. Leaf, (Retired)
Director, Test and Evaluation
HQ USAF/TE
1650 Air Force Pentagon
Washington, DC 20330-1650

Mr. Larry Lynn
Director
DARPA/DIRO
3701 North Fairfax Drive
Arlington, VA 22203-1714

Dr. John Lyons
Director of Corporate Laboratory
US Army Laboratory Command
2800 Powder Mill Road
Adelphi,MD 20783-1145

Col Ed Mahen
DARPA/DIRO
3701 North Fairfax Drive
Arlington, VA 22203-1714

Dr. Arthur Manfredi
OSWR
Washington, DC 20505

Dr George Mayer
Office of Director of Defense
Reserach and Engineering
Pentagon, Room 3D375
Washington, DC 20301-3030

Dr Bill Murphy
ORD
Washington, DC 20505

Dr Julian C Nall
Institute for Defense Analyses
1801 North Beauregard Street
Alexandria, VA 22311

DISTRIBUTION LIST

Dr Ari Patrinos [5]
Associate Director for
Biological and Environmental Reserach
ER-70
US Department of Energy
1901 Germantown Road
Germantown,MD 207874-1290

Dr Bruce Pierce
USD(A)D S
The Pentagon, Room 3D136
Washington, DC 20301-3090

Mr John Rausch [2]
Division Head 06 Department
NAVOPINTCEN
4301 Suitland Road
Washington, DC 20390

Records Resource
The MITRE Corporation
Mailstop W115
1820 Dolley Madison Blvd
McLean,VA 22102

Dr Victor H Reis [5]
US Department of Energy
DP-1, Room 4A019
1000 Independence Ave, SW
Washington, DC 20585

Dr Fred E Saalfeld
Director
Office of Naval Research
800 North Quincy Street
Arlington, VA 22217-5000

Dr Dan Schuresko
O/DDS&T
Washington, DC 20505

Dr John Schuster
Technical Director of Submarine
and SSBN Security Program
Department of the Navy OP-02T
The Pentagon Room 4D534
Washington, DC 20350-2000

Dr Michael A Stroscio
US Army Research Office
P. O. Box 12211
Research Triangle NC27709-2211

Ambassador James Sweeney
Chief Science Advisor
USACDA
320 21st Street NW
Washington, DC 20451

Dr George W Ullrich [3]
Deputy Director
Defense Nuclear Agency
6801 Telegraph Road
Alexandria, VA 22310

Dr. David Whelan
Director
DARPA/TTO
3701 North Fairfax Drive
Arlington, VA 22203-1714

Dr Edward C Whitman
Dep Assistant Secretary of the Navy
C3I Electronic Warfare & Space
Department of the Navy
The Pentagon 4D745
Washington, DC 20350-5000